Estonian Journal of Earth Sciences
2026, **75**, 2, 122–147

https://doi.org/10.3176/earth.2026.08

www.eap.ee/earthsciences
Estonian Academy Publishers

RESEARCH ARTICLE

Received 15 February 2026
Accepted 23 April 2026
Available online 1 October 2026

Keywords:
SWAN, Delft3D, model comparison, fetch-based models, nearshore wave climate

Corresponding author:
Rain Männikus
rain.mannikus@taltech.ee

Citation:
Männikus, R., Soomere, T., Suursaar, Ü. and Chien, H. 2026. Where can simple wave models replace sophisticated ones in the Gulf of Riga? *Estonian Journal of Earth Sciences*, **75**(2), 122–147. https://doi.org/10.3176/earth.2026.08

© 2026 Authors. This is an open access article distributed under the terms and conditions of the Creative Commons Attribution (CC BY) license (http://creativecommons.org/licenses/by/4.0).

Where can simple wave models replace sophisticated ones in the Gulf of Riga?

Rain Männikus[a], Tarmo Soomere[a,b], Ülo Suursaar[c,d] and Hwa Chien[e]

[a] Wave Engineering Laboratory, Department of Cybernetics, School of Science, Tallinn University of Technology, Ehitajate tee 5, 19086 Tallinn, Estonia

[b] Estonian Academy of Sciences, Kohtu 6, 10130 Tallinn, Estonia

[c] Estonian Marine Institute, Faculty of Science and Technology, University of Tartu, Mäealuse 14, 12618 Tallinn, Estonia

[d] Institute of Ecology, School of Natural Sciences and Health, Tallinn University, Narva mnt 29, 10120 Tallinn, Estonia

[e] Institute of Hydrological and Oceanic Sciences, National Central University, 300 Jhongda Rd., Jhongli District, 320317 Taoyuan City, Taiwan

ABSTRACT

We address the options for reconstructing time series of wave parameters in coastal areas with complex bathymetry and geometry by means of contemporary high-resolution multi-nested spectral wave model SWAN forced with wind information from the ERA5 reanalysis, a similar model in the Delft3D suite forced with one-point wind data, and a parametric fetch-based wave model forced with one-point wind data recorded in the neighbourhood of the locations of interest. The focus is on the Gulf of Riga and Moonsund in the West Estonian Archipelago in the eastern Baltic Sea. The SWAN model and its implementation in the Delft3D suite are applied with up to five nesting levels to explore the match between the modelled and recorded wave heights during 15 multi-month (up to two-year-long) measurement sessions at 14 locations ranging over the years 2006–2024, with a model resolution down to 11 m. The data from seven sites are presented for the first time. None of the models properly replicates wave properties at all locations. The SWAN model forced with ERA5 winds shows better performance than the simpler models at relatively open locations. The model forced with one-point wind data shows a better match with the recorded data at more nearshore locations with complex bathymetry and geometry. The simple fetch-based model forced with one-point wind data shows comparable performance at such locations. The presented results make it possible to specify the range of applicability of contemporary wave models in regions with complex geometry and provide guidance on the selection of wind information for fetch-based express models.

1. Introduction

Successful coastal design and management substantially rely on the correct assessment of local wave parameters that actually impact man-made structures and shape the shores. However, their specification is challenging in water bodies with complex geometry, such as the Great Lakes (Lu et al. 2026), the Mediterranean Sea (Barbariol et al. 2021), the North Sea (Groll and Weisse 2017), or the Baltic Sea (Björkqvist et al. 2017; Adell et al. 2023). While offshore wave fields are usually relatively homogeneous and vary insignificantly over a distance of a few miles, local bathymetry and coastline geometry often induce substantial spatial variability in nearshore wave properties (Hanes and Erikson 2013; Soomere et al. 2020). This challenge is exacerbated in semi-sheltered water bodies of elongated shape, such as the Baltic Sea, and especially its sub-basins, such as the Gulf of Finland (Pettersson et al. 2010; Suursaar 2013). Another common reason for the complexity of the wave climate in such areas is its highly intermittent nature, with long calm periods being interrupted by sequences of storms (Soomere and Eelsalu 2014; Soomere 2023).

The situation is further complicated by the possible (mis)match between the geometry of the basin and the direction of moderate and strong winds. This feature, well-known in the Baltic Sea and the Great Lakes, gives rise to a strong dependence of wave properties not only on wind speed but even more on wind direction (Suursaar 2015; Männikus et al. 2024a, 2024b; Lu et al. 2026). The resulting spatially

highly inhomogeneous Baltic Sea wave climate (Soomere and Räämet 2011; Björkqvist et al. 2018) is jointly shaped by the complex bathymetry and coastline and bidirectional structure of moderate and strong winds (Soomere 2001, 2003). It becomes most clearly evident in elongated sub-basins of the sea. While southwesterly winds are most common in the open part of the Baltic Sea (Baltic Proper), unusually intense waves with a significant wave height of 8.1 m were excited in 2019 in the Sea of Bothnia by northerly winds with a 10-min speed of up to 32.5 m/s (Björkqvist et al. 2020). Even though easterly winds are usually infrequent and relatively weak in the Baltic Sea basin, the all-time maximum significant wave height of 5.2 m (first recorded in 2001) was repeated in the Gulf of Finland during an easterly storm in 2012 (Pettersson et al. 2013). On top of that, complex local geometry and bathymetry may substantially add to the spatio-temporal variability of wave properties via geometric sheltering (Caliskan and Valle-Levinson 2008) and/or steering (Hanes and Erikson 2013; Männikus et al. 2022) and focusing effects (e.g. Salonen and Rautenbach 2021).

A natural outcome of the situation described above is that hindcast wave properties produced by even the most contemporary high-resolution wave models driven by high-quality reconstructions of wind fields may deviate substantially from in situ recorded wave parameters in many areas (Giudici et al. 2023). Moreover, rare extremes that occur during storms with winds from unusual directions are not always well represented in recorded wave parameters (Soomere et al. 2008). In such situations, the most reliable approach to evaluating average and extreme wave properties and associated forces at a single location is to perform extensive in situ measurements. This is often not feasible because such estimates are usually needed at short notice. The existing long-term instrumental wave recordings that can be used to estimate extreme wave loads are usually performed at a few sites far from the locations of coastal engineering structures. This is the case even in water bodies that have a relatively dense marine observation network, such as the Baltic Sea (She et al. 2020).

As a result, offshore wave climates are adequately replicated using properly calibrated numerical wave models. Contemporary wave models, such as SWAN or WAM, forced with state-of-the-art modelled wind data, such as the more local BaltAn65+ dataset (Björkqvist et al. 2018) or the global ERA5 reanalysis (Giudici et al. 2023), replicate offshore wave properties well. Only in nearshore areas does the use of different wind forcings lead to a certain difference in the statistics of higher wave conditions (Giudici et al. 2023). However, models that perform well in open-sea areas do not always adequately replicate wave properties in the nearshore with a complex coastline and highly variable bathymetry. Even the most advanced models that are forced with state-of-the-art modelled information and carefully calibrated using (usually offshore) wave measurements (Björkqvist et al. 2018; Giudici et al. 2023) often show an extensive mismatch between the modelled and recorded wave properties in the nearshore of the Baltic Sea (Giudici et al. 2023; Najafzadeh et al. 2024). It is not clear whether the mismatch is caused by shortcomings in the wind forcing (Viigand et al. 2026), the inability of wave models to replicate wave transformation in areas with complex bathymetry and geometry, or a mismatch between measurement locations and the wave model grid cells (Najafzadeh et al. 2024).

A feasible way forward is to additionally calibrate and verify such wave models using local wave measurements. This is realistic for Estonian coastal waters, where many short-term instrumental wave recordings have been performed since 2002. The first such attempts used a pressure-based wave recorder and covered only a few days in Tallinn Bay (Soomere and Rannat 2003) or to the east of Naissaar in the Gulf of Finland (Soomere et al. 2008). Further campaigns employed more advanced devices, such as a downward-looking echosounder (Didenkulova 2011), a bottom-mounted acoustic Doppler current profiler (ADCP) (Suursaar and Kullas 2009; Suursaar 2013), or surface buoys (Männikus et al. 2024a), and provided time series of wave properties over a few months at several locations in the nearshore of the eastern Baltic Proper, the Gulf of Riga, and the Gulf of Finland. A device (SmartBuoy) that estimated wave properties using a pressure sensor has been deployed near Skulte in the southeast of the Gulf of Riga since 2020 (Eelsalu et al. 2025).

A challenge for coastal engineers in this context is the development of rapid and inexpensive but still adequate first-level estimates of typical and extreme wave properties at potential locations of different engineering structures. The time scale of such exercises often leaves little time for model calibration, verification, and sensitivity analyses (Männikus et al. 2024a). The use of simple parametric wave models that are adjusted to replicate the complex geometry may provide a first-order solution. Such models using, e.g., Sverdrup–Munk–Bretschneider-type formulations (e.g. USACE 1984) are based on robust physics. Even though they ignore some processes, such as refraction, shoaling, or energy exchange between wave components, they provide realistic estimates of wave properties in smaller and reasonably deep basins where the contribution of nonlinear interactions is less significant. It is thus expected that, e.g., wave hindcasts in the nearshore of the Harilaid Peninsula (northwestern Saaremaa, at a location that is fully open to the predominant wind directions in the northern Baltic Proper; Fig. 1) generated by a locally calibrated fetch-based model forced with high-quality recorded wind data from the vicinity match well with the outcome of the SWAN model driven by ERA5 winds (Suursaar et al. 2014; Männikus et al. 2024a).

Intriguingly, the performance of simple models forced with high-quality one-point winds in the spirit of Soomere (2005) and Suursaar (2013, 2015) was basically the same or even better in terms of significant wave heights at several locations along the southern nearshore of the Gulf of Finland (Männikus et al. 2024a). The same conjecture held for the northeastern Baltic Proper. The core component of the good performance of such models is the availability of high-quality in situ (preferably) offshore wind data at a reasonable distance (up to about 100 km) from the location of interest. The performance of these models was lower when the wind was aligned with the axis of the Gulf of Finland. A likely reason for this feature was the strong dependence of the fetch length

on the wind direction in this elongated gulf. It is thus natural to assume that such simple models may perform even better in areas with a more regular shape.

In this study, we focus on the semi-enclosed, relatively small sub-basin of the Baltic Sea, the Gulf of Riga, and the adjoining smaller basin called the West Estonian Archipelago Sea (Moonsund, Väinameri; Fig. 1). The Gulf of Riga measures roughly 140 × 150 km and has a surface area of 17 913 km^2. Its average and maximum depths are 26 m and 66 m, respectively (Stiebrins and Väling 1996; Skudra and Lips 2017). Moonsund has dimensions of approximately 50 × 50 km, a surface area of 2243 km^2, and is even shallower, with an average depth of 4.7 m. These sub-basins are connected to each other and to the Baltic Proper through several narrow straits. Unlike the Gulf of Finland, the Gulf of Riga has a mostly regular, oval-like shape. Due to its semi-enclosed nature, waves from the Baltic Proper may have a limited impact only on its northern segment (Suursaar et al. 2012; Najafzadeh et al. 2024). It has a short fetch (less than 150 km) for the predominant wind and wave directions from the southwest, west, and northwest or north-northwest (Eelsalu and Soomere 2026). The coastline in the western, southern, and eastern parts of the gulf (i.e. mostly the Latvian side) is almost straight or gently curved (Tsyrulnikov et al. 2008). The northern and northeastern coastal areas of this gulf and the entire Moonsund are heavily indented by small peninsulas, islets, and shallow bays.

We employ for comparison instrumentally recorded wave properties from 15 multi-month, up to two-year-long measurement campaigns at 14 different sites ranging over the

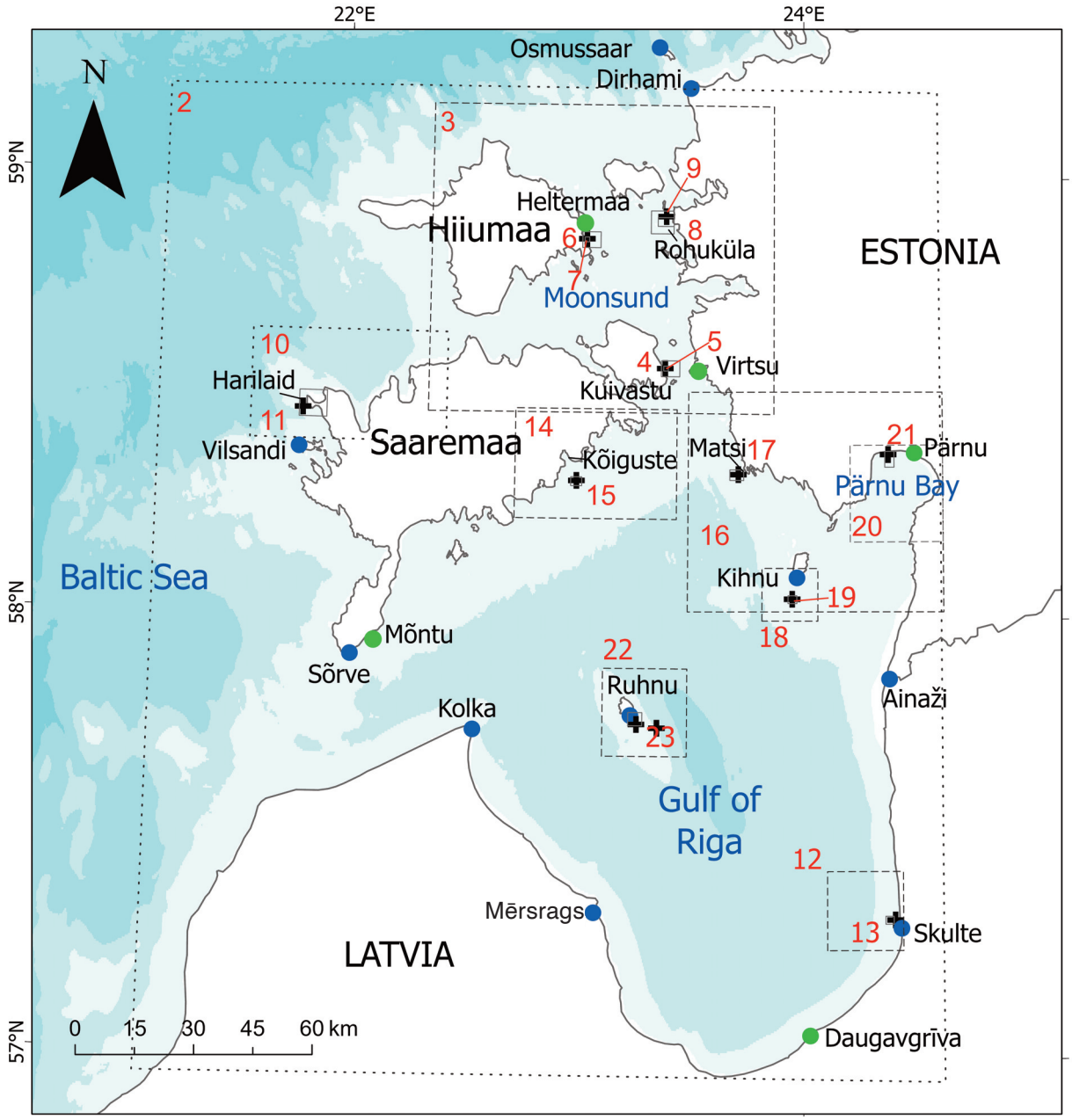

Fig. 1. Wave (black crosses), wind (blue circles), and water level (green circles) measurement locations in the Gulf of Riga and Moonsund. Black rectangles with red numbers denote second-, third-, fourth-, and fifth-level grids of the SWAN model. The resolution of each grid and the number of grid cells are presented in Table 1.

years 2006–2024. This set involves all known wave measurements in Moonsund, the Estonian waters of the Gulf of Riga, and near Skulte in Latvian waters (Fig. 1). We also include the results of wave measurements at two sites near the Harilaid Peninsula in the western nearshore of Saaremaa (Fig. 1). The results from five sites (Harilaid, Kõiguste, Matsi, Kihnu, and Skulte) have been either partially (Skulte) or fully (the other sites) used to verify the implementation of the SWAN model for the entire Baltic Sea (Giudici et al. 2023) and for the Gulf of Riga (Najafzadeh et al. 2024). The data from the other four sites (Valgerand, Pärnu, and two locations near the Port of Ruhnu) have been used fully or partially for local case studies (Männikus et al. 2024b; Tõnisson et al. 2024). The data from three campaigns (Rohuküla, Heltermaa, and Kuivastu) are presented for the first time.

The core research questions are: (i) whether any of the implemented models is able to adequately replicate recorded wave properties at all measurement locations, at least in terms of basic statistical properties, such as bias, root mean square difference, and correlation coefficient, and also in terms of the reproduction of wave properties in the strongest storms; (ii) which one-point wind information is the best for the replication of wave properties; (iii) whether a simple fetch-based model performs satisfactorily enough to be used as an express tool; and (iv) whether there are locations where none of the models performs well. We also explore the ranking of the models at different sites.

We begin with a description of recorded wind and water level data in the vicinity of the measurement locations and the different wave models used in the analysis. Two of the models used are versions of the state-of-the-art spectral wave model SWAN. Both are implemented at high resolution, down to approximately 50 m and even less, with nesting up to the fifth level. One of them is forced with wind information from the ERA5 reanalysis. The other version, implemented in the Delft3D (D3D) suite, is forced with locally recorded one-point wind data. This model is intentionally used without any tuning. A simple fetch-based semi-empirical wave model is also forced with local one-point wind data. All calculations are performed for an idealised ice-free situation. First, we explore which wind information and mode of calculation (stationary or non-stationary) lead to the best performance of models forced with one-point wind data. Based on this selection, we compare the outputs of multiple wave models with recorded wave properties at all locations. Furthermore, we analyse the ability of all models to reproduce wave properties in the strongest wave storms. Finally, we discuss the models' performance from different perspectives, analyse and comment on their capacity to reconstruct wave properties at locations of different types, and formulate the main messages from the analysis.

2. Data and methods

2.1. Modelled wind data

The wind forcing for our reconstructions is taken from the ERA5 dataset (Hersbach et al. 2020), a fifth-generation global atmospheric reanalysis produced by the European Centre for Medium-Range Weather Forecasts (ECMWF 2016), covering the period from 1979 to the present and updated quarterly. ERA5 is based on a more recent release of the ECMWF Integrated Forecast System (IFS cycle 41r2; ECMWF 2016) than its predecessors and provides enhanced temporal sampling as well as finer horizontal and vertical resolutions (1 h, 0.25°, and 137 vertical levels, respectively) (Hersbach et al. 2020). Hourly near-surface wind speed and direction are calculated for the wave model from the 10 m u- and v-wind components provided by Hersbach et al. (2018).

This wind information is not perfect in either global (Bessonova et al. 2025) or local applications (Viigand et al. 2026). Because of its moderate spatial resolution, it has inherent uncertainties in coastal areas where local topography and underlying surface contrasts are not fully captured. The ERA5 wind data tend to underestimate extreme wind speeds (Sheridan et al. 2022; Gandoin and Garza 2024; Afolabi et al. 2025), especially during the morning hours in the Baltic Sea (Borsche et al. 2016). This feature naturally leads to a certain underestimation of wave heights near coastal areas (Giudici et al. 2023). Moreover, ERA5 tends to overestimate very low wind speeds in the Gulf of Riga (Viigand et al. 2026).

Despite these shortcomings, the overall performance of the ERA5 wind data is generally strong compared with that of other higher-resolution models for the Baltic Sea (Borsche et al. 2016). It exhibits highly realistic spatial and temporal variability: both wind speed and direction vary adequately across the domain and throughout the simulation period. Even though there are several wind datasets for the Baltic Sea, some of them with higher resolution than ERA5, such as the Uncertainties in Ensembles of Regional Reanalysis (UERRA) atmospheric reanalysis (Ridal et al. 2017) or the Copernicus European/Arctic Regional Reanalysis (CERRA, CARRA2) available from the Copernicus C3S services, we prefer ERA5 because it has finer temporal resolution (1 h) than, e.g., CARRA2. Furthermore, its use makes our study comparable with previous efforts in wave modelling in the study area. Based on the extensive comparison of modelled and recorded wave properties at several locations in the Gulf of Riga (Najafzadeh et al. 2024), we treat wave properties reconstructed using the SWAN model (Booij et al. 1999) as implemented in Giudici et al. (2023) and Najafzadeh et al. (2024) and forced with the ERA5 wind fields as the 'virtual ground truth'. In other words, we employ time series of wave properties reconstructed in this manner as a reference against which all other model simulations are assessed.

2.2. The SWAN model forced with modelled wind data

The SWAN model (Booij et al. 1999) is a third-generation phase-averaged spectral wave model developed at Delft University of Technology. Giudici et al. (2023) and Najafzadeh et al. (2024) implemented a three-level nested scheme of this model using regular rectangular grids. The first-level grid covered the entire Baltic Sea with a modest resolution of 3 nautical miles (nmi, 1 nmi = 1852 m; approximately 5500 m). The results were used as boundary conditions for

finer second-level grids. One of these grids covered the Gulf of Riga and surrounding areas with a resolution of 1 nmi. The third-level grids (Fig. 1) focused on coastal areas in the Gulf of Riga and Moonsund, with a resolution ranging from 260 to 560 m, depending on the properties of the shallow-water bathymetry and shoreline geometry (Najafzadeh et al. 2024). Wave properties from the second-level grid were used as boundary information for the third-level grid. More detailed information about the model set-up, calibration, and validation is provided in Giudici et al. (2023) and Najafzadeh et al. (2024).

In this study, we constructed additional grids (up to the fifth level) in nearshore areas (Fig. 1; Table 1) near available instrumental wave measurement sites. The nesting scheme relies on previous experience (e.g. Tõnisson et al. 2024) and the bathymetry in the boundary areas. The ratio of the size of cells of the first- and second-level grids is 3:1, which is usual in such exercises. This ratio is larger, up to 7.4:1, for the second- and third-level grids because, owing to the regular shape and smooth offshore bathymetry of the Gulf of Riga and the western nearshore of the West Estonian Archipelago, the properties of modelled wave fields vary slowly at the borders of the third-level grids (cf. Najafzadeh et al. 2024). The borders of the additional grids are also chosen in relatively deep areas where the wave properties vary insignificantly between cells of the relevant lower-level grid. This feature suggests that a ratio of up to 25:1 between the size of cells of grids at different levels is still acceptable.

As the typical depth of some selected areas was just a few metres, the frequently occurring water level variations of more than 1 m in this region (Männikus et al. 2022) may considerably alter wave transformation in shallow areas. To reflect this feature, we employed recorded water level data from nearby tide gauges. These readings were applied homogeneously to the entire set of grids. Doing so made it possible to consider the varying water level during strong preconditioning events (Andrée et al. 2023) and during some storms in the domain where most of the waves arriving at the selected locations were generated. This adjustment had almost no effect on the outcome of simulations with the 3 nmi grid for the entire Baltic Sea but had a clear impact on the results of calculations using higher-resolution grids. Furthermore, different parameters were used in multiple set-ups to detect their influence on the results. The information about bathymetry was obtained from the databases of the Estonian Transport Administration (Peeter Väling, pers. comm., February 2020), the Latvian Institute of Aquatic Ecology (Maris Skudra, pers. comm., February 2020), and the Baltic Sea Bathymetry Database of the Baltic Sea Hydrographic Commission (BSHC 2013). Hereafter, we refer to this model as the SWAN/ERA5 suite.

2.3. Recorded wind and water level data

The above-described modelled wind data and multi-nested wave model form a complicated and computationally demanding system that needs extensive calibration and verification. It can be effectively used for studies of offshore wave climate, its extremes, and specific features (Männikus et al. 2022; Najafzadeh et al. 2024). However, it is not realistic to implement such a system for assessing the local wave climate at high resolution at short notice. A feasible alternative is to use locally measured one-point wind information to force simpler

Table 1. Computational grids for the SWAN/ERA5 suite and Delft3D suite. See Fig. 1 for grid locations

No.	Name of the grid	No. of cells	Resolution, °	Cell size, m	Nested in	Level
1	Baltic Sea	210 × 249 = 52 290	0.1 × 0.05	5500	–	1
2	Gulf of Riga	113 × 150 = 16 950	0.03 × 0.015	1700	Baltic Sea	2
3	Moonsund	300 × 280 = 84 000	0.005 × 0.0025	290	Gulf of Riga	3
4	Kuivastu Large	100 × 90 = 9000	0.0008 × 0.0004	50	Moonsund	4
5	Kuivastu	100 × 110 = 11 000	0.0002 × 0.0001	11	Kuivastu Large	5
6	Heltermaa Large	100 × 90 = 9000	0.0008 × 0.0004	50	Moonsund	4
7	Heltermaa	100 × 110 = 11 000	0.0002 × 0.0001	11	Heltermaa Large	5
8	Rohuküla Large	130 × 130 = 16 900	0.0008 × 0.0004	50	Moonsund	4
9	Rohuküla	180 × 200 = 36 000	0.0002 × 0.0001	11	Rohuküla Large	5
10	NW Saaremaa	170 × 100 = 17 000	0.005 × 0.0025	290	Baltic Sea	2
11	Harilaid	150 × 150 = 22 500	0.0008 × 0.0004	50	NW Saaremaa	3
12	Skulte Large	80 × 90 = 7200	0.004 × 0.002	230	Gulf of Riga	3
13	Skulte Small	90 × 90 = 8100	0.0004 × 0.0002	24	Skulte Large	4
14	Laimjala	140 × 100 = 14 000	0.005 × 0.0025	290	Gulf of Riga	3
15	Kõiguste	130 × 100 = 13 000	0.0004 × 0.0002	24	Laimjala	4
16	Pärnu	110 × 100 = 11 000	0.01 × 0.005	570	Gulf of Riga	3
17	Matsi	150 × 120 = 18 000	0.0004 × 0.0002	20	Pärnu	4
18	Kihnu Large	60 × 60 = 3600	0.004 × 0.002	240	Gulf of Riga	3
19	Kihnu	90 × 90 = 8100	0.0004 × 0.0002	24	Kihnu Large	4
20	Pärnu Bay	100 × 110 = 11 000	0.004 × 0.002	230	Gulf of Riga	3
21	Valgerand	90 × 180 = 16 200	0.000 × 0.0002	24	Pärnu Bay	4
22	Ruhnu Large	90 × 100 = 9000	0.004 × 0.002	230	Gulf of Riga	3
23	Ruhnu	150 × 150 = 22 500	0.0004 × 0.0002	24	Ruhnu Large	4

wave models (e.g. Männikus et al. 2024a, 2024b). In this study, we use wind data from selected Estonian and Latvian coastal weather stations located in the vicinity of the wave measurement sites and operated by the Estonian Environment Agency (EEA 2025) and the Latvian Environment, Geology and Meteorology Centre (LEGMC 2025).

The key question in selecting a suitable weather station is how well the records from the station represent marine winds. Coastal wind properties are usually affected by topography and by contrasts in the properties of the surrounding landscape (see the relevant analysis for some Estonian coastal stations in Keevallik et al. 2007; Žukova 2009). This feature makes some sources almost unusable (Keevallik 2003). We tried out as many one-point wind datasets as possible for forcing the wave model. By calculating bias (Δ), root mean square deviation (D_{rms}), and the correlation coefficient (R) between modelled and recorded wave properties, we selected the most suitable wind forcing for the simpler models (the D3D suite and SPM model) at each measurement location. Time series of wave properties generated using these wind data were used for further comparisons.

To specify the most suitable wind information for each selected area, we employed all available wind datasets from meteorological stations on the islands of the Gulf of Riga (Kihnu and Ruhnu), in the coastal zone of the Gulf of Riga and Moonsund, and from two locations to the north of the study area at the entrance to the Gulf of Finland, one of them on the mainland (Dirhami) and the other on the island of Osmussaar. Here, we briefly describe the main features of these weather stations (Fig. 1) and their recordings that were not included in previous analyses (Männikus et al. 2024a, 2024b).

Since autumn 2003, weather stations operated by the EEA have been equipped with MILOS-520 automatic devices that record hourly wind speed and direction at a resolution of 0.1 m s^{-1} and 1°, respectively. The Osmussaar station is located on the northwestern tip of Osmussaar (Fig. 1). Judging by the topography, its recordings of easterly and southeasterly winds are apparently influenced by the island. The Dirhami station is located in a local port and is open to the north and northwest. Winds from other directions are sheltered by the forest. The Vilsandi meteorological station is located on a small island to the west of Saaremaa. The data from Vilsandi are often used as a standard, high-quality representation of wind properties in the northern Baltic Proper (Soomere 2003; Suursaar and Kullas 2009; Suursaar 2013). This dataset is highly reliable except for easterly winds (Soomere 2001), which are generally less frequent and weaker than the predominant southwesterly or north-northwesterly winds in this region. The Sõrve station is located at the tip of the Sõrve Peninsula at the southern end of Saaremaa and is open to all directions. Its recordings are influenced by the peninsula to the north of the station. The Virtsu station operates in a village adjacent to the sea, where the recorded wind properties are influenced by nearby houses and trees. The most open direction is the north-northwest. The Ruhnu station, active since 1958, is located in the southern part of the island, about 200 m from the sea. It is open to all directions, except to the north and northeast, where forest grows. In a similar manner, the Kihnu station is sheltered by the forest in the north and east.

Latvian coastal meteorological stations near the Gulf of Riga (Ainaži, Skulte, Mērsrags, and Kolka) are located approximately 1 km inland from the coast, where the wind properties are evidently influenced by surrounding houses and trees. The hourly records used for modelling waves at Skulte (after 1 July 2020) have a temporal resolution of 0.1 m s^{-1} and directional resolution of 1°.

Water level recordings were taken from the Estonian Weather Service and Latvian Environment, Geology and Meteorology Centre databases from 1 January 2006 to 31 December 2024. The stations (Heltermaa, Virtsu, Pärnu, Ruhnu, Kihnu, and Mõntu in Estonia, and Daugavgrīva in Latvia) were selected based on data completeness (Männikus et al. 2020) and the distance from the wave measurement locations. The hourly data are in the European Vertical Reference System. A detailed overview of the water level recording sites and the recorded data is given in Männikus et al. (2020) and Männikus and Soomere (2023).

2.4. Two versions of the Delft3D model forced with one-point wind data

Version 40.11 of the SWAN model in the D3D (WAVE 2013) suite was employed to replicate waves under unidirectional homogeneous (one-point) wind conditions applied to all grid levels. The model was run either in stationary or non-stationary mode with respect to the use of wind information. In stationary mode, it is assumed that the instantaneous wind properties have been present for a long time and that the wave parameters at each time instant represent a fully developed sea. This approach is acceptable if the travel time of waves from the generation area to the coast is relatively small compared with the time scale of variations in the wave field (WAVE 2013). It is also acceptable when the 'memory' of wave fields is shorter than the temporal resolution of wind information. In non-stationary mode, the actual variation in wind properties (the duration of wind and its temporal resolution, here: 1 h) is taken into account. The wave field replicated by the model in this mode might not be fully developed and may represent an intermediate time instant during the storm (WAVE 2013).

We employed the same set of computational grids (Fig. 1) that was created for the SWAN/ERA5 suite. The forcing (one-point) wind was chosen based on recorded wind data from nearby meteorological stations. As mentioned above, the recorded values of the water level from nearby stations were used to replicate the impact of water level variations on modelled wave data in shallow areas. This model is denoted as the D3D suite.

2.5. Fetch-based SPM model

Semi-empirical (parametric) wave models, applied in wave studies and in coastal engineering since the 1950s, provide properties of waves that reflect fully developed wave fields

for the given wind speed and fetch length. While being easy to set up and computationally efficient, their primary limitation in basins with complex coastlines and bathymetry is the accuracy of the representation of the effective fetch length for each wind direction. Conventionally, the fetch length is defined as the upwind distance to the nearest shoreline for a given wind direction, although in some cases algorithms have been introduced to account for basin characteristics over a broader wind sector (Tolvanen and Suominen 2005; Massel 2013). Despite their simplicity, these models produce reasonably accurate results, particularly in (semi-) enclosed, medium-sized water bodies (Seymour 1977; Huttula 1994), where wave field memory is relatively short. Inspired by this approach, Suursaar and Kullas (2009) and Suursaar (2013) developed a calibration framework for SPM models in the Estonian coastal sea, allowing the model to function as a 'virtual' extension of fixed-point observational records, using wind data from a nearby weather station. Applying an iterative calibration procedure, this method usually required a modification of the fetch length for some directions to mimic the impact of the complex coastline and numerous islands on wave propagation and transformation (e.g. Suursaar et al. 2012).

To emulate this computationally efficient approach, we adopt the methodology described by Kamphuis (2010) and hereafter refer to it as the SPM model, based on formulations from the Shore Protection Manual (USACE 1984). The fetch length (from the point of interest to the closest shoreline or larger island) is evaluated within ±11° directional sectors from the main directions of the 16-rhumb system using a custom MATLAB script, which also calculates the mean water depth from the available bathymetric dataset and water level data. Wave parameters were estimated by applying recorded wind properties from a nearby meteorological station. Unlike in Männikus et al. (2024a), hourly significant wave height (H_S) and peak period (T_p) were evaluated in both stationary and non-stationary modes. Wave growth during a rotation of the wind direction was considered by limiting the changes to ±22.5° compared with the wind properties at the previous time instant. Intentionally, no model calibration or wind speed adjustment was performed. On the contrary, the SPM model was intended to represent generic locations and non-specific applications. Consequently, it was expected that these uncalibrated, simplified model results would be substantially less accurate than those obtained from purpose-built, calibrated simulations such as those presented by Suursaar (2013, 2015).

2.6. Wave measurements

We employed in the analysis the results of all available professional wave measurements from 2006 to 2024 in the coastal sea of Moonsund and the Gulf of Finland and near the western shore of Saaremaa (Table 2). They are unevenly distributed in time: one campaign was performed in 2006–2007, four in 2010–2013, and the rest in 2020–2024, actually covering less than half of the years from 2006 to 2024. A detailed overview of the measurement locations, instruments employed, and earlier use of the wave data is presented in the Appendix.

Scatter diagrams of in situ estimated and numerically replicated H_S values suggest that the modelled and recorded wave heights generally match each other fairly well under relatively low and moderate wave conditions when $H_S \leq 0.5$ m (Fig. 2). The match between these values is much worse under higher wave conditions $H_S > 0.5$ m and poor if $H_S > 1$ m in relatively sheltered locations, such as Valgerand. For this reason, we exclude from further analysis (i) time instants with recorded $H_S > 1$ m in the sheltered conditions of Rohuküla (Moonsund) and Valgerand (Pärnu Bay), and (ii) instants with recorded $H_S > 1.5$ m at Kõiguste and Matsi in shallow-water regions of the northern Gulf of Riga (Table 2). As the dataset contains only a few such entries at Matsi, about 10 at Valgerand and Pärnu, and 20–40 at Kõiguste and at two locations in Rohuküla, doing so has an insignificant effect on the stat-

Table 2. Location and timing of wave measurements used in the analysis

No.	Location	Abbr.	N coordinate	E coordinate	Start	End	Depth, m	Device
1	RohukülaNBW	RoN	58.9097	23.4155	11.06.2021	23.11.2022	4.0	Pressure sensor
2	RohukülaS	RoS	58.9016	23.4189	15.10.2021	23.11.2022	4.5	Pressure sensor
3	RohukülaST	RoST	58.9028	23.4193	29.08.2023	05.11.2023	4.5	Wave buoy
4	Heltermaa	Hel	58.8670	23.0496	07.06.2022	31.12.2024	5.0	Echosounder
5	Kuivastu	Kui	58.5736	23.3966	28.04.2023	31.12.2024	6.5	Echosounder
6	Harilaid	Ha07	58.4667	21.8167	20.12.2006	23.05.2007	14.0	RDCP-600
7	Harilaid	Ha13	58.4667	21.8500	26.10.2013	31.10.2013	14.0	RDCP-600
8	Kõiguste	Koi	58.3167	23.0167	02.10.2010	04.05.2011	11.5–12.7	RDCP-600
9	Matsi	Mat	58.3333	23.7167	13.06.2011	03.09.2011	9.6–10.2	RDCP-600
10	Kihnu	Kih	58.0500	23.9500	10.09.2012	15.05.2013	10.7–12.1	RDCP-600
11	Valgerand	Val	58.3622	24.3721	09.11.2021	28.11.2022	1.5	Wave buoy
12	Pärnu Bay	Par	58.3836	24.3672	09.11.2021	28.11.2022	4.0	Wave buoy
13	Ruhnu Port	Rpor	57.7782	23.2754	03.05.2021	01.05.2023	4.6	Wave buoy
14	Ruhnu Sea	Rsea	57.7695	23.3420	03.05.2021	18.11.2021	19.0	Wave buoy
15	Skulte	Sku	57.3195	24.3858	21.07.2020	29.01.2022	15.0	Wave buoy

Table 3. Basic statistics of wave properties at the measurement sites. Red numbers indicate estimates that are likely contaminated by single erroneous recordings. Records that correspond to table cells with a red background were excluded from further analysis, as they are most likely incorrect. The 99.9th percentile and the maximum H_S value are most likely incorrect at Heltermaa and Kuivastu. From the entire pool of recorded data, only records on the full hour (or closest to the full hour if more than one entry was recorded) are considered in the analysis

Location	H_S threshold, m				H_S percentiles, m						
	0	0.5	1.0	1.5	50	90	95	99	99.5	99.9	100
Harilaid 2007	3691	1590	717	218	0.40	1.29	1.55	2.05	2.24	2.98	3.16
Harilaid 2013	2327	1044	412	100	0.42	1.22	1.45	1.99	2.18	2.87	3.40
Kõiguste	1718	576	219	26	0.26	1.07	1.22	1.54	1.75	1.93	1.96
Matsi	1941	452	100	5	0.11	0.84	1.01	1.34	1.44	1.53	1.63
Kihnu	5897	1863	783	161	0.10	1.10	1.33	1.71	1.80	2.06	2.32
Valgerand	2466	391	11	0	0.19	0.56	0.67	0.91	0.98	1.19	1.21
Pärnu Bay	2671	483	13	0	0.24	0.60	0.70	0.90	0.99	1.26	1.28
Ruhnu Port	12 791	4184	858	87	0.36	0.87	1.08	1.43	1.56	1.75	2.02
Ruhnu Sea	9516	4791	1890	422	0.50	1.27	1.47	1.80	1.98	2.29	2.45
Skulte	26 823	10 693	3755	1315	0.39	1.16	1.49	2.24	2.55	3.17	3.77
RohukülaNBW	19 488	402	13	7	0.07	0.32	0.41	0.57	0.64	0.88	3.02
RohukülaS	7488	276	0	0	0.08	0.36	0.46	0.73	0.80	0.92	0.98
RohukülaST	3083	469	41	0	0.23	0.57	0.72	1.05	1.10	1.31	1.41
Heltermaa	70 052	3600	1377	687	0.08	0.34	0.51	1.48	2.01	2.81	3.20
Kuivastu	50 087	5069	950	170	0.12	0.50	0.67	1.24	1.40	2.59	5.21

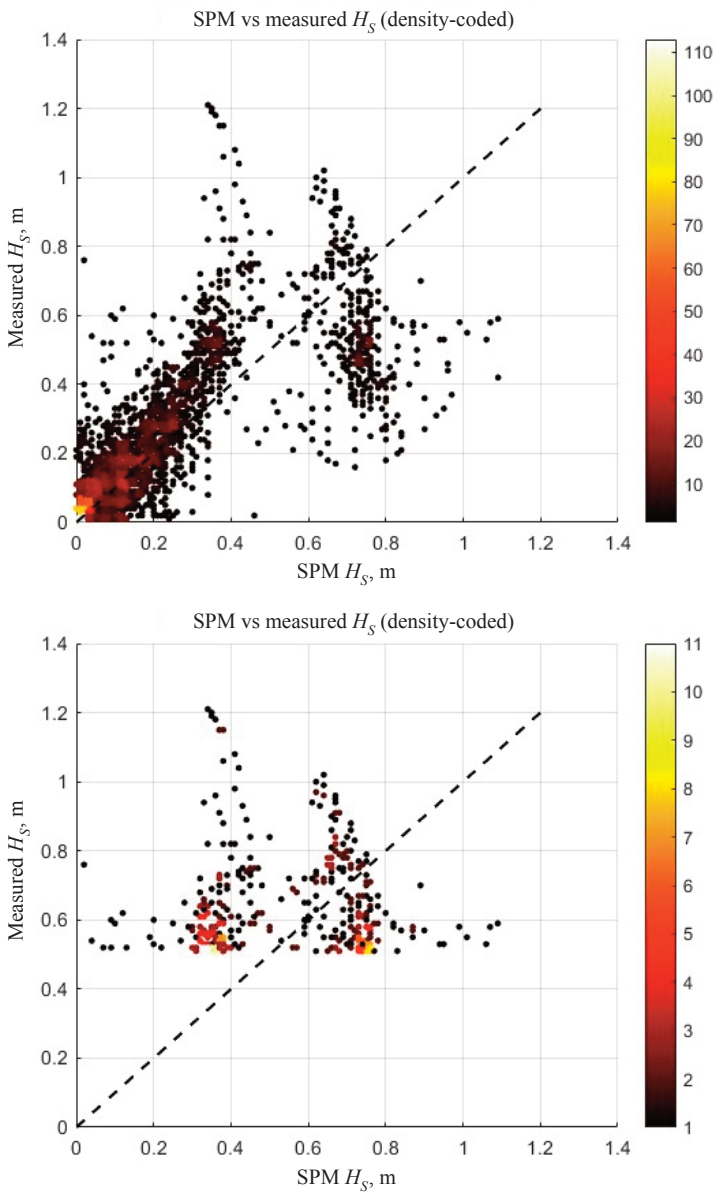

Fig. 2. Top panel: scatter diagram of all recorded hourly values of H_S and H_S evaluated using the SPM model at Valgerand (Fig. 1). Lower panel: the same, but only for recorded H_S > 0.5 m.

istical properties of the relevant datasets. This operation only removes the unrealistic highest quantile of H_S at RohukülaNBW.

3. Results

The performance of the models was assessed by comparing hourly wave properties calculated using the SWAN/ERA5 and D3D suites and the SPM model in and around the Gulf of Riga (Fig. 1) with the results of in situ wave measurements. The main focus is on significant wave height H_S, but peak periods T_p are also briefly discussed.

First, we present and discuss the modelling results obtained using the D3D suite and SPM model at every measurement location. The goal is to select the wind information and the mode of its use that lead to the best fit between modelled and recorded wave properties. Thereafter, we discuss differences between the resulting values and the results of the SWAN/ERA5 suite, as well as differences between the modelled and recorded wave properties, to estimate the performance of the models. As low wave heights under weak winds are always adequately represented by all models in relatively small water bodies, we focus on situations with substantial wave activity, specifically, on wave conditions where the recorded $H_S \geq 0.5$ m. We intentionally use this fixed threshold to avoid a spurious match between the modelled and recorded wave properties in more sheltered locations where low wave heights prevail and the use of a fixed percentile may distort the comparison. We also address all wave fields and wave conditions with H_S exceeding 1 m and 1.5 m at some locations. The use of the threshold $H_S \geq 0.5$ m inter alia excludes situations with total or partial ice cover when our model (that ignores sea ice) projects substantial waves that actually do not exist or are much lower. We treat a positive bias as showing that the modelled H_S values exceed the recorded H_S values.

3.1. Appropriate forcing at different measurement locations

Statistical properties of the match between reconstructed and recorded wave heights are used to select the most suitable wind information for the D3D suite and SPM model (Table 4) for the entire duration of the measurement campaigns (Table 2). To avoid a spurious match between low wave heights, we use only time instants with recorded wave heights $H_S \geq 0.5$ m in this subsection.

We describe the results in the sequence of openness of the measurement sites. Near the location that is most open to the predominant wind and wave direction, **Harilaid**, the (Acoustic) Doppler Current Profiler (RDCP) was placed at two different locations (Ha07 in 2006–2007 and Ha13 in 2013; Fig. 1). For both campaigns (Table 2), the D3D suite was forced with wind data from the two closest locations, Vilsandi and Sõrve, and run in both stationary and non-stationary modes. On the one hand, the best match with the recorded wave properties in 2007 was obtained when the suite was forced with Vilsandi wind data and run in stationary mode (Table 4). On the other hand, in 2013, when the RDCP was placed closer to the coast, the best match was obtained with simulations in stationary mode forced with Sõrve wind data. The runs in non-stationary mode forced with wind data from Sõrve and Vilsandi in 2013 yielded similar R values, but a larger bias (about –0.6 m) and higher D_{rms} (0.63 m). Hence, the use of non-stationary wind data leads to an underestimation of wave heights.

Kõiguste and Matsi represent two relatively sheltered locations in the northern nearshore of the Gulf of Riga where the contribution from northerly waves is negligible. The closest sites of wind information are Ruhnu and Kihnu and the two locations mentioned above, Sõrve and Vilsandi. At **Kõiguste** (Koi), we modelled wave properties using five runs of the D3D suite: in stationary and non-stationary modes forced with wind data from Vilsandi, and in stationary mode forced with wind data from Sõrve, Ruhnu, and Kihnu. The best match with recorded wave heights was obtained when the suite was forced with wind information from Ruhnu (Table 4). The use of stationary mode and wind information from Vilsandi and Sõrve yielded a similar quality of match to that obtained using the Kihnu wind data. The use of the latter data led to a lower bias ($\Delta = 0.02$ m) but much larger root mean square difference ($D_{rms} = 0.42$ m) and weaker correlation ($R = 0.28$). Calculations with the SPM model led to a slightly better match when the model was employed in non-stationary mode and forced with wind data from Ruhnu, compared with the run in stationary mode using wind data from the same location.

At **Matsi** (Mat), we reconstructed wave properties using eight runs of the D3D suite: in stationary and non-stationary modes forced with wind data from Vilsandi, Ruhnu, Sõrve, and Kihnu. Somewhat surprisingly, the run in stationary mode with wind data from Sõrve gave the best match with recorded wave heights. The use of stationary mode and wind data from Ruhnu led to an underestimation of wave heights. Computations with the SPM model showed that the use of stationary mode and wind data from Ruhnu led to a better match than the use of wind data from Sõrve. At this location, the difference between runs in non-stationary and stationary modes was larger than in the situations described above (Table 4).

Kihnu and Ruhnu are small islands offshore in the Gulf of Riga. Ruhnu is fully open in all directions, whereas Kihnu is located in the northeast of the gulf and thus is partially sheltered from northerly winds and waves. The closest sites providing wind information are the islands themselves and Sõrve. At **Kihnu** (Kih), wave properties were modelled using six runs of the D3D suite: in both stationary and non-stationary modes forced with wind data from Ruhnu, Sõrve, and Kihnu. The best match with the measurements was provided by simulations in stationary mode forced with wind data from Kihnu (Table 4). The application of the SPM model in stationary mode with wind information from Ruhnu led to a somewhat better match, primarily in terms of D_{rms} than its application in non-stationary mode with wind data from the same location. Simulations forced with wind data from other stations resulted in considerably higher bias and D_{rms}, and lower R.

The match between wave heights replicated using the D3D suite with different wind forcings and recorded data at the Port of **Ruhnu** (Rpor) and at a depth of 19 m near the is-

Table 4. Selected winds and modes of computation that provide the best match between recorded and modelled wave properties. The smaller numbers of datapoints compared with Table 3 indicate that only the measurements on full hours were included in the comparison

No.	Location	Abbr.	No. of datapoints	SWAN/ERA5	Best wind data and mode in D3D	Best wind data and mode in SPM
				Δ, m / D_{rms}, m / R for $H_S \geq 0.5$ m		
Location open to the Baltic Proper						
1	Harilaid 2007	Ha07	3668	0.35/0.52/0.75	Vilsandi stationary 0.06/0.63/0.56	Vilsandi stationary 0.21/1.03/0.43
2	Harilaid 2013	Ha13	2323	–0.01/0.18/0.92	Sõrve stationary 0.24/0.42/0.82	Sõrve stationary 0.15/0.43/0.82
Partially sheltered locations in the north of the Gulf of Riga						
3	Kõiguste	Koi	1672	0.20/0.28/0.74	Ruhnu stationary –0.05/0.25/0.68	Ruhnu non-stationary 0.29/0.45/0.68
4	Matsi	Mat	1739	0.12/0.22/0.71	Sõrve stationary 0.03/0.32/0.60	Ruhnu stationary 0.13/0.33/0.49
Small islands in the Gulf of Riga						
5	Kihnu	Kih	3913	0.22/0.32/0.78	Kihnu stationary 0/0.36/0.64	Ruhnu stationary 0.06/0.29/0.65
6	Ruhnu Port	Rpor	7308	0.11/0.22/0.80	Ruhnu stationary –0.30/0.35/0.83	Ruhnu non-stationary –0.07/0.29/0.76
7	Ruhnu Sea	Rsea	3825	0.02/0.19/0.86	Ruhnu stationary –0.50/0.56/0.69	Ruhnu stationary –0.33/0.48/0.58
Locations in the interior of Pärnu Bay						
8	Valgerand	Val	2456	–0.22/0.24/0.69	Kihnu stationary –0.11/0.17/0.61	Kihnu stationary –0.12/0.26/0.04
9	Pärnu Bay	Par	2457	–0.17/0.20/0.65	Kihnu stationary 0.02/0.15/0.62	Ruhnu non-stationary –0.01/0.37/0.48
Open location in the southeast of the Gulf of Riga						
10	Skulte	Sku	13402	–0.28/0.39/0.81	Vilsandi stationary –0.18/0.53/0.56	Vilsandi stationary –0.08/0.55/0.55
Locations in Moonsund						
11	RohukülaNBW	RoN	4872	–0.15/0.33/–0.14	Dirhami stationary –0.03/0.29/0.19	Dirhami non-stationary 0.11/0.32/0.28
12	RohukülaS	RoS	1872	0.03/0.14/0.36	Dirhami stationary –0.04/0.20/0.60	Dirhami non-stationary 0.14/0.25/0.43
13	RohukülaST	RoST	2501	–0.14/0.20/0.69	Osmussaar stationary –0.08/0.19/0.70	Dirhami non-stationary 0/0.32/0.39
14	Heltermaa	Hel	11225	–0.77/0.96/–0.06	Osmussaar stationary –0.47/0.77/–0.01	Osmussaar non-stationary –0.15/0.82/0.03
15	Kuivastu	Kui	8886	–0.29/0.36/0.66	Osmussaar stationary –0.31/0.40/0.54	Osmussaar non-stationary –0.18/0.49/0.50

land of Ruhnu (Rsea) was analysed in Männikus et al. (2024b). The use of stationary mode and wind data from Ruhnu led to the best match between the recorded and modelled data for both the D3D suite and the SPM model (Table 4). The use of wind data from Ruhnu to force the D3D suite in non-stationary mode led to a value of R similar to that for a similar run in stationary mode, but both the bias and D_{rms} were about 0.15 m higher. Runs in both stationary and non-stationary modes led to an underestimation of wave heights. For the SPM model, the use of stationary mode and wind data from Ruhnu led to a better match than the application of any other wind datasets or modes. The presented characteristics of the match (Table 4) are better than those provided in Männikus et al. (2024b) because of the use of an improved algorithm for evaluating the fetch and a correction for water depth as described above.

The measurement locations at **Valgerand** (Val) and **Pärnu** (Par) are located in the interior of Pärnu Bay and are open only to a narrow range of wind and wave directions from the south-southwest. The closest source of wind information is Pärnu, but we also employed wind data from Kihnu, Ruhnu, Sõrve, and Vilsandi to perform ten runs of the D3D suite in both stationary and non-stationary modes forced with wind data from all five sites. Consistent with Tõnisson et al. (2024), the best match with the recorded data was obtained when the suite was run in stationary mode, forced with wind data from Kihnu (Table 4). The SPM model failed to accurately reproduce wave parameters at Valgerand but achieved a better match with recorded data at Pärnu when wind data from Ruhnu were employed. These results suggest that fetch-based models generally cannot adequately reproduce wave parameters in embedded bays such as Pärnu Bay,

and especially in relatively sheltered locations, such as Valgerand, where the correlation between modelled and recorded wave heights is non-existent, even when the formal bias and D_{rms} are modest.

Skulte (Sku) is located in the southeast of the Gulf of Riga and is thus mostly affected by northerly waves because the fetch length for waves from the southwest is only 10–20 km. Wave properties were modelled using six runs of the Delft3D suite: in both stationary and non-stationary modes forced with wind data from Ruhnu, Vilsandi, and Sõrve. The best match was achieved in a run in stationary mode forced with wind data from Vilsandi (Table 4). The use of other winds led to substantial underestimation of even reasonably high waves ($H_S \geq 1$ m and $H_S \geq 1.5$ m). The bias reached –0.49 m, $D_{rms} > 0.92$ m, and the correlation was non-existent ($R < 0.09$). The use of stationary mode led to a better match than non-stationary mode in all explored cases.

We also employed wind information from Ainaži, Skulte, Mērsrags, Kolka, and Kihnu to force the SPM model at Skulte. Interestingly, the use of wind data from any of the Latvian stations led to a clear underestimation of wave heights at this site. It is likely that this feature reflects the relatively sheltered locations of these meteorological stations, where the local wind speed is lower than offshore. The best match was obtained when the SPM model was run in stationary mode and forced with wind data from Vilsandi, although even in this case wave heights were underestimated.

Rohuküla and Heltermaa are located in Moonsund and Kuivastu in the Suur Strait, which connects the Gulf of Riga with Moonsund, but at a location sheltered from waves excited in the Gulf of Riga. The closest meteorological stations that are open to winds in the Baltic Proper are Osmussaar and Dirhami, but we also employed data from Vilsandi for Heltermaa and Kuivastu. Wave properties at three locations near **Rohuküla** (RoN, RoS, and RoST) were evaluated using the D3D suite run in stationary and non-stationary modes forced with Vilsandi wind data, and in stationary mode forced with Osmussaar and Dirhami wind data. The difference between wave properties evaluated using the suite in stationary and non-stationary modes and the recorded values was insignificant at all measurement locations. Such small differences combined with a weak correlation partially reflect relatively low wave intensity: the measured H_S values were less than 1.5 m. At two locations near Rohuküla (RoN and RoS), the D3D suite run in non-stationary mode and forced with Dirhami wind data yielded the best match with the recorded wave heights (Table 4), while the use of Osmussaar wind data tended to overestimate wave heights. At the third location at Rohuküla (RoST), simulations using Osmussaar wind data gave the best match with the recorded data (Table 4), while simulations using Dirhami wind data clearly underestimated wave heights. The reasons for the relatively large differences between the properties of the modelled and recorded data at these locations might be the different time periods and devices used for the measurements. Namely, at RoN, the values of R were below 0.21 for all employed wind datasets.

At **Heltermaa** (Hel) and **Kuivastu** (Kui), we used four different runs of the D3D suite: in stationary and non-stationary modes with wind data from Vilsandi, and in stationary mode with wind data from Osmussaar and Dirhami. The overall properties of waves replicated using Osmussaar wind data had the best match with the results of measurements at both locations (Table 4). Similar to the above, the difference between the indicators of the match between recorded wave heights and wave properties reconstructed by the suite in stationary and non-stationary modes using wind data from Vilsandi was small. It is likely that the locations of the wave gauges at the eastern tips of the quays (Photos A1 and A2 in the Appendix) were such that some wave heights were overestimated (Table 2). The most likely reason is that strongly reflecting structures may lead to an up to twofold increase in wave heights and possibly also to splashes in their immediate vicinity. This feature explains the frequent presence of unexpectedly high H_S recordings (especially at Heltermaa; Table 2), which were not visible in the modelled time series. We chose not to remove such instances from the dataset (clear sudden peaks, etc.) because they only appeared for waves from a narrow range of directions, and compared the datasets 'as is'.

Table 4 provides a list of variations in the model set-up and wind forcing that led to the best match between the simulated and recorded wave properties at individual measurement locations. On the one hand, the results suggest that, intriguingly, in the Gulf of Riga, the D3D suite run in stationary mode is more suitable for evaluating wave parameters than the same model employed in non-stationary mode. On the other hand, the SPM method in non-stationary mode leads to a better match at some locations than similar simulations in stationary mode. A comparison of this outcome for the larger Gulf of Riga and the smaller Moonsund suggests that the non-stationary mode of the SPM model performs better in more enclosed areas and semi-open bays with a rugged coastline (Fig. 3). The best match for relatively open locations usually occurs when local wind data are employed, while the best match for more sheltered locations is often provided by winds from a meteorological station that is open to the Gulf of Riga or the Baltic Proper.

Figure 3 shows the statistical properties for recorded $H_S \geq 0.5$ m in a Taylor diagram. The clustering of markers representing different models is apparent and hints at their preferred practical uses, including the conjecture that the SPM model often works reasonably well at locations that are relatively open to medium-sized water bodies. The clear outlier is the marker that reflects the results of the SPM model at Harilaid (Ha13). A likely reason is that the SPM model assumes that the fetch length is equal to the sea size, which is not always the case.

3.2. Replication of significant wave heights

To obtain a wider picture of the quality of wave reconstructions using the SWAN/ERA5 and D3D suites with the wind information that gives the best match for wave conditions with $H_S \geq 0.5$ m (Table 4), and the SPM model with

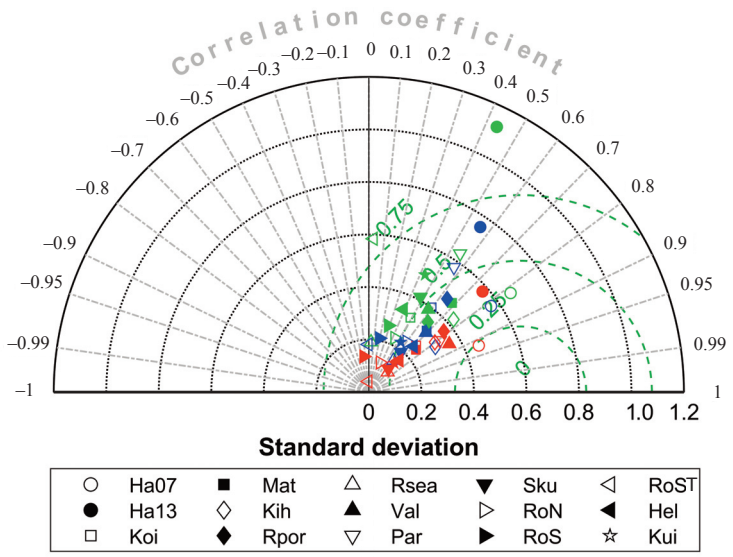

Fig. 3. Taylor diagram quantifying the degree of correspondence between the modelled and recorded significant wave heights $H_S \geq 0.5$ m (Table 4). Red markers indicate the SWAN/ERA5 suite, blue markers indicate the D3D suite, and green markers indicate the SPM model. The dashed line indicates centred D_{rms}. For abbreviations, see Table 2.

similar wind information, we analysed the bias, D_{rms}, and R between the recorded and reconstructed wave properties for all waves (i.e., recorded $H_S \geq 0$ m) and for higher waves (recorded H_S exceeding 0.5 m, 1 m, or 1.5 m). The analysis using higher thresholds was conducted only if there were more than 100 hourly recordings exceeding the threshold (Table 3). As above, a positive bias means that the modelled H_S values are higher than the recorded H_S values. The comparison is presented, as above, starting with the most open sites.

The best match with measurements in open regions at **Harilaid** (Ha07 and Ha13) is provided by wave heights reconstructed using the SWAN/ERA5 suite (Table 4). The resulting statistical properties differ from those provided by Najafzadeh et al. (2024). Their simulations led to a better match than our calculations at Ha07 and to a worse match at Ha13. A likely reason is that they used a coarser Gulf of Riga grid with a resolution of about 1700 m (Table 1), while we employed a finer grid to replicate wave heights at this location. The use of 1 nmi grid cells may result in the choice of different grid cells to represent the locations Ha07 and Ha13, which are 1950 m apart from each other. Männikus et al. (2024a) chose the same grid cell to represent wave properties at both locations. The match with the results of the D3D suite was slightly worse. The use of the SPM model led to the worst match. The selection of the threshold for H_S (0, 0.5, 1.0, or 1.5 m) significantly affected the statistical properties of the match between the results of the SPM model and wave measurements but had almost no effect on these properties for the match between the results of the other models and wave measurements.

The use of the SWAN/ERA5 or D3D suite led to the best match between recorded and modelled wave heights at semi-sheltered locations. As the wave measurement site at **Kõiguste** (Koi) was in water 11.5 m deep, the adjustment of the water level did not affect wave heights in simulations with the SWAN/ERA5 suite. Najafzadeh et al. (2024) reported a slightly smaller bias and D_{rms} (by about 0.03 m) and a stronger correlation between the results of measurements and their simulations than we obtained in our simulations. The reason might be that a coarser grid (a cell size of about 260 m in Najafzadeh et al. 2024, while the cell size in our simulations was about 24 m) gave results for a slightly different location in Najafzadeh et al. (2024). A comparison of the results of the SWAN/ERA5 suite with those of the D3D suite and the SPM model shows that the best match at this location is provided by the D3D suite run in stationary mode and forced with wind data from Kihnu (Table 4). The use of the SWAN/ERA5 suite led to a slightly stronger correlation ($R = 0.78$) but overestimated wave heights. This overestimation was stronger for lower waves ($H_S < 0.5$ m), evidently because pressure-based wave recognition may have missed some of the energy of shorter waves.

In contrast, the use of the SWAN/ERA5 suite yielded the best match with measurements at **Matsi** (Mat; Table 4). The use of the D3D suite in stationary mode forced with wind data from Sõrve, and the SPM model in stationary mode forced with wind data from Ruhnu overestimated wave heights and showed much larger scatter. The difference between the performance of these models was clearer in the time series of H_S (not shown here). As at Kõiguste, water level fluctuations had no effect on the wave heights simulated using the SWAN/ERA5 suite in this relatively deep (9.6 m) location. The statistical properties of the match between simulated and measured H_S (bias, D_{rms}, and R) coincide with those reported in Najafzadeh et al. (2024).

Similar to the situation at Kõiguste, the D3D suite run in stationary mode and forced with wind data from Kihnu performed best at **Kihnu** (Kih; Table 4). Although the match between the results of the SWAN/ERA5 suite and recorded H_S has a smaller D_{rms} and R, it has a relatively large bias. The results of the SPM model run in non-stationary mode forced

with Ruhnu wind data show a similar match with wave measurements in terms of these statistical parameters, but a slightly worse match than the results of the D3D suite. This shows the potential for tuning the SPM model towards an implementation that could efficiently reproduce wave heights. Here too, Najafzadeh et al. (2024) reported a slightly smaller bias and D_{rms} (about 0.03 m) and a stronger correlation. The reason might be the same as at Kõiguste.

The use of the SWAN/ERA5 suite results in a larger bias (0.11 m vs 0.06 m) and D_{rms} (0.22 m vs 0.14 m) and a lower R (0.80 vs 0.92) between modelled and recorded waves for all wave heights at the **Port of Ruhnu** (Rpor) than the similar values reported in Männikus et al. (2024b). The difference stems from the different time periods used in the comparisons: in our analysis, the measurements from 2023 are also considered. The larger values of the bias and D_{rms} may also be caused by slightly different locations of the centre of the model grid cell and the measurement site. Still, the use of the SWAN/ERA5 suite provides the best match with the recorded data. Surprisingly, the D3D suite gives the worst match, while the SPM model run in non-stationary mode and forced with wind data from Ruhnu yields acceptable results. The same gradation holds for simulations at the **Ruhnu Sea** (Rsea) location. The statistical properties of the match between the results of the SWAN/ERA5 suite and the recorded values are the same as those reported in Männikus et al. (2024b). It is natural that individual values of H_S, especially those that are >1 m, have a much larger spread at a deeper sea location than at a more confined shallow-water location near the port.

The best match between simulated and recorded H_S at the most sheltered sites, Valgerand and Pärnu, is provided by the D3D suite run in stationary mode and forced with wind data from nearby Kihnu. The use of the SPM model led to the worst match with recorded wave properties, most likely because of its inability to replicate enhanced refraction of waves in shallow water. The SWAN/ERA5 suite underestimates wave heights in shallow **Pärnu Bay** (Par), which has a typical depth of about 4–5 m.

We briefly examined options for achieving a better match between the results of the SWAN/ERA5 suite and the recorded data at these two locations by considering the effect of changing (i) the wind parameterisation recommended by Wu (1982) to the default one in the SWAN model, (ii) the whitecapping dissipation coefficient (C_{ds2}), (iii) the values of the breaking constants α and γ, and (iv) wave growth modes. The simulations were performed for one month in 2021 at both locations. It is expected that increasing the breaking constants (allowing higher waves to propagate into shallow water) has the largest effect on the model output. Still, the largest recorded H_S (1.2 m) remained underestimated (0.8 m) in the output of all versions of the resulting SWAN/ERA5 suite.

The use of the SWAN/ERA5 suite underestimates H_S at **Skulte** (Sku). The highest simulated H_S was 2.5 m, whereas the recorded maximum H_S was about 3.7 m. The bias and D_{rms} are larger when only higher waves are considered (–0.71 m and 0.77 m for waves with $H_S \geq 1.5$ m). Najafzadeh et al. (2024) reported a lower bias and D_{rms}, but they considered a nine-month period (July 2020–April 2021). For waves with $H_S \geq$ 0.5 m, the bias and D_{rms} reported by Najafzadeh et al. (2024) are higher than in our study. The smallest underestimation of H_S is obtained in simulations using the D3D suite and the SPM model run in stationary mode and forced with wind data from Vilsandi. However, these results have a higher spread (larger D_{rms}) and weaker correlation (R = 0.55) than wave properties reconstructed using the SWAN/ERA5 suite. The core outcome of this comparison is the conjecture that modelling waves at Skulte requires more model tuning than at other locations.

The best modelling results near the **Port of Rohuküla** are provided by the D3D suite. The SPM model performs slightly better than the SWAN/ERA5 suite at RoN but produces clearly worse results at the more southern locations, RoS and RoST. As expected, correlation coefficients between the recorded and reconstructed wave heights are larger for all models when lower waves are taken into account. The situation is more complicated for the biases and D_{rms} values. These are larger at RoS for all waves compared with the situations when only higher waves are considered. This pattern is reversed at the other nearby locations, RoN and RoST. A comparison of the bias, D_{rms}, and R at these sites reveals a higher spread of H_S values at RoN and RoS. A likely reason is that a pressure sensor was used to record the waves at RoN and RoS, whereas a more reliable industrial wave buoy recorded waves at RoST.

The D3D suite yields a better match with measurements performed using the echosounder at **Heltermaa** (Hel) than the SWAN/ERA5 suite. The match is poor for both modelling environments for the higher waves (the correlation between the modelled and recorded data is non-existent) but is better when all wave recordings are considered. A likely reason for this feature is that very few moderate or strong winds bring high waves to this port. The majority of such winds blow from the southwest or north-northwest, directions from which the vicinity of the Port of Heltermaa is sheltered. Only winds from the east may bring large waves to the port structures. Such waves experience strong reflection and often create splashes at the measurement location. This feature is not replicated by phase-averaged (SWAN) and parametric (SPM) models. It is thus natural that the largest recorded H_S values considerably exceed the corresponding modelled values.

Although a similar set-up with an echosounder was used at **Kuivastu** (Kui), the match between the modelled and recorded wave heights is clearly better. The use of the SWAN/ERA5 suite leads to the best match. The match with the results of the D3D suite is only slightly worse. The SPM model provides a clearly worse match at Kuivastu and Heltermaa. As the measurement set-up at Kuivastu is similar to that at Heltermaa, it is expected that the modelled H_S values are somewhat underestimated; however, the difference is unexpectedly large. A likely reason is that Kuivastu is more open to northern directions. Winds from these directions often bring relatively high waves to the Port of Kuivastu. These waves are recorded adequately and form a notable part of the recordings.

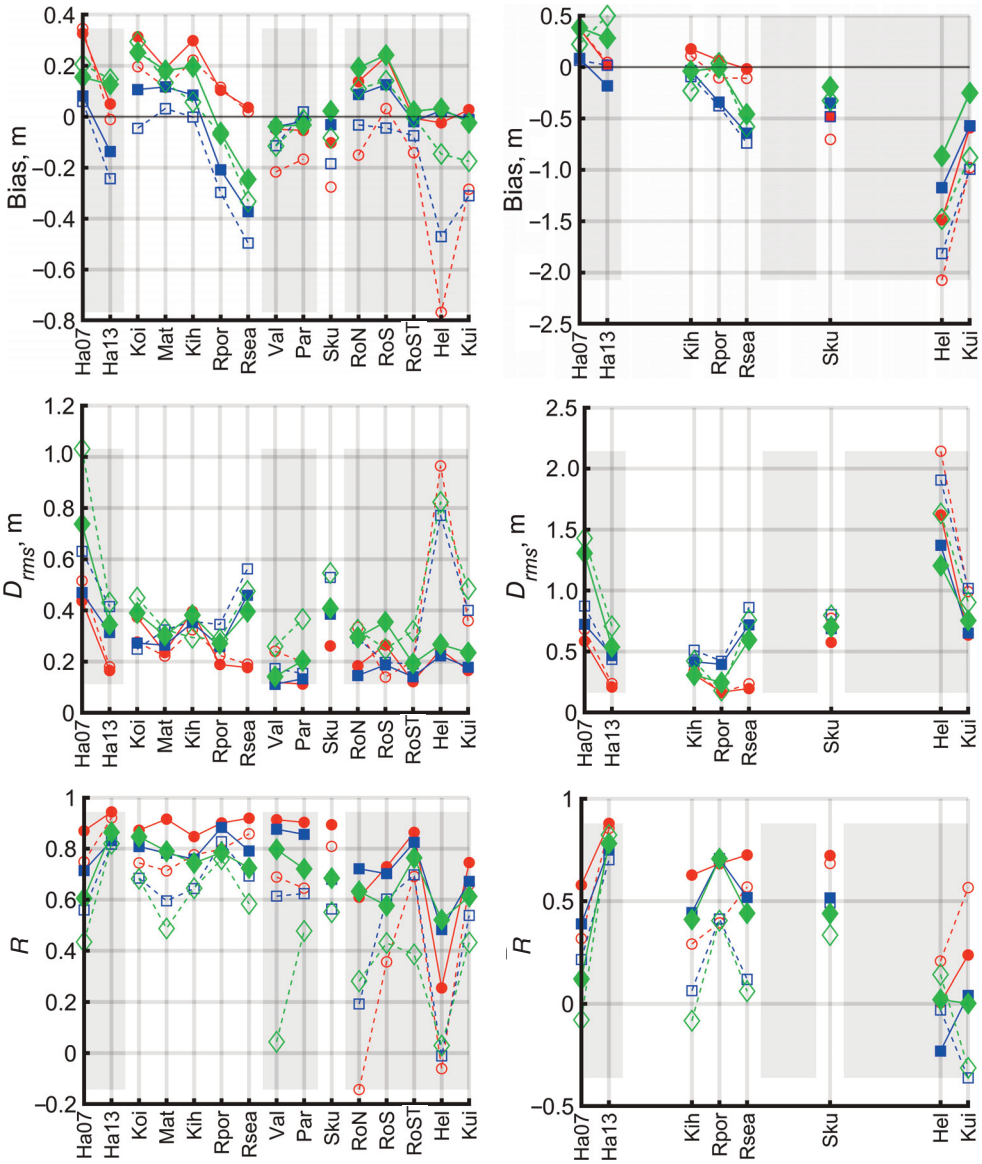

Fig. 4. Bias (upper panels), D_{rms} (middle panels), and correlation coefficient R (lower panels) of the recorded and modelled H_S values. Left panels: all wave conditions (continuous lines with filled markers) and recorded waves with $H_S \geq 0.5$ m (dashed lines). Right panels: wave conditions with $H_S \geq 1$ m (continuous lines with filled markers) and $H_S \geq 1.5$ m (dashed lines). Red circles: outputs modelled using the SWAN/ERA5 suite; blue squares and green diamonds: outputs of the D3D suite and the SPM model, respectively, both forced with one-point wind data listed in Table 4. Wave measurement sites Ha07 and Ha13 are located in the nearshore of the Baltic Proper; Koi, Mat, Kih, Val, Par, Rpor, and Rsea are located in the interior of the northern Gulf of Riga; Sku is located in the southeastern Gulf of Riga; RoN, RoS, and Hel are located in Moonsund; and Kui is located in the Suur Strait between the Gulf of Riga and Moonsund. A positive bias means that the modelled H_S values exceed the recorded values. For abbreviations, see Table 2.

3.3. Replication of wave periods

The SWAN/ERA5 suite replicates recorded peak periods T_p better than the other models at almost all locations in terms of bias, D_{rms}, and R (Fig. 5). This feature apparently replicates its ability to consider the shape of the basin and the actual wind pattern. The match between the recorded data and the results of using the D3D suite is slightly better at locations in Moonsund (RoN, RoS, RoST, Hel, and Kui). Its rather small area (short fetch and possibly faster wave growth because of more turbulent wind) plays a role in this feature. The R values between the recorded and simulated T_p are smaller than those for H_S values. The bias between the recorded T_p values and those reconstructed using the SPM model is comparable with, and sometimes smaller, than that for values replicated using the D3D and SWAN/ERA5 suites. However, the corresponding values of D_{rms} and R are higher and lower, respectively (Fig. 5).

There is no clear pattern of over- or underestimation of peak periods among the three models. The signs of the biases in the estimated periods at Ha07, Ha13, Rpor, Rsea, and Sku signal that wave periods in more exposed areas tend to be overestimated. Strikingly high D_{rms} at Harilaid (Ha07 and Ha13) in the nearshore of the Baltic Proper compared with other locations suggests that the D3D suite and the SPM model with default settings overestimate wave periods in areas open to the Baltic Proper, most likely because the actual strong wind fields do not cover the entire Baltic Proper, where wave fields are not always fully developed. Männikus et al. (2024a)

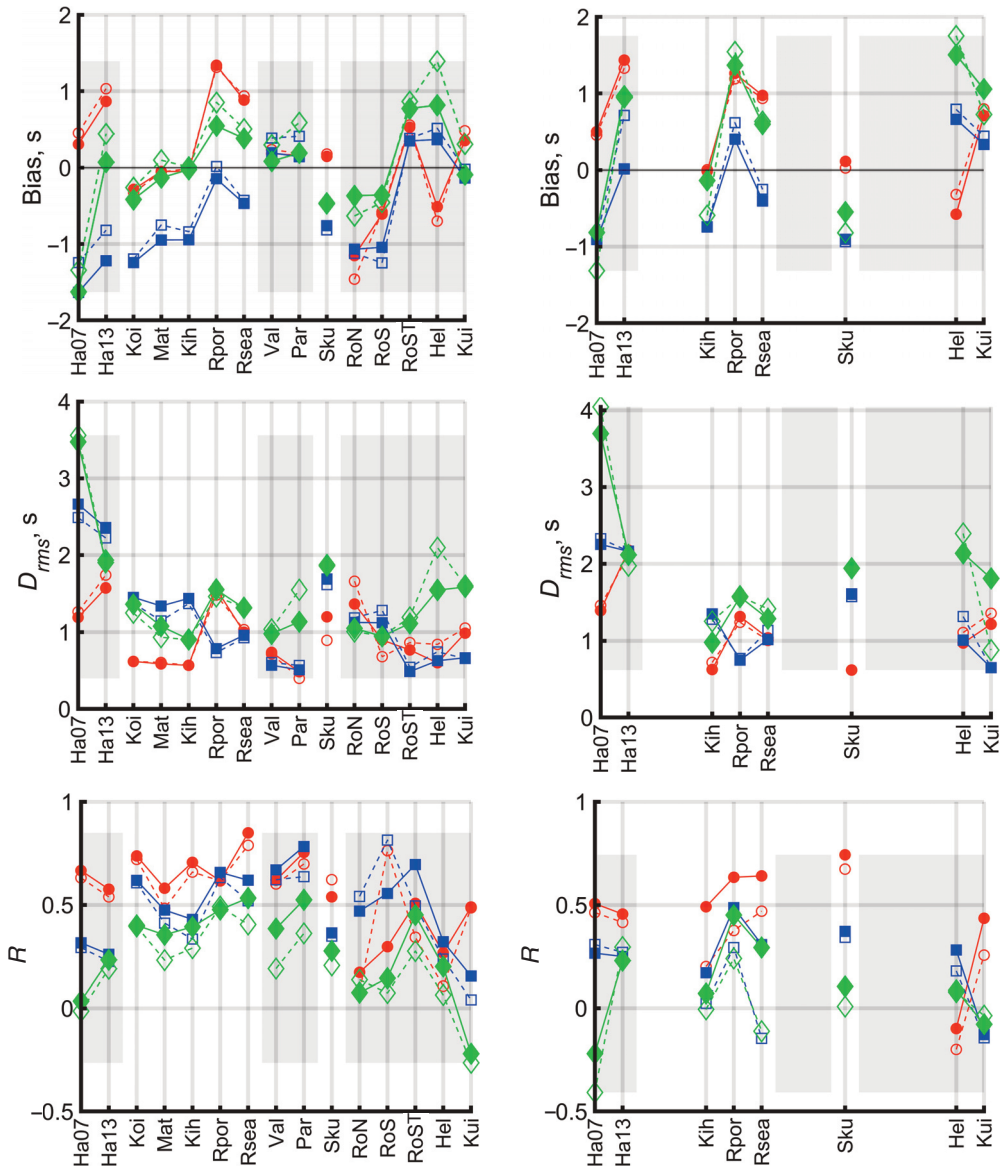

Fig. 5. Bias (upper panels), D_{rms} (middle panels), and correlation coefficient R of the recorded and modelled T_p values. Left panels: recorded waves with $H_S \geq 0.5$ m (continuous lines with filled markers) and $H_S \geq 0.5$ m (dashed lines). Right panels: recorded waves with $H_S \geq 1$ m (continuous lines with filled markers) and $H_S \geq 1.5$ m (dashed lines). Red circles: outputs modelled using the SWAN/ERA5 suite; blue squares and green diamonds: outputs of the D3D suite and the SPM model, respectively, both forced with one-point wind data listed in Table 4. A positive bias means that the modelled T_p values exceed the recorded values. For abbreviations, see Table 2.

analysed the Ha07 and Ha13 datasets together and found similar values for different thresholds of wave heights. Locations in the Gulf of Finland showed about the same or higher D_{rms} and R. Thus, the openness of the particular location plays a significant role in correctly assessing wave periods.

Najafzadeh et al. (2024) reported for Ha07 $\Delta = 0.18$ s, $D_{rms} = 1.42$ s, and $R = 0.62$, and for Ha13 $\Delta = 0.41$ s, $D_{rms} = 1.46$ s, and $R = 0.56$ for all wave conditions. We obtained $\Delta = -0.21$ s, $D_{rms} = 1.50$ s, and $R = 0.57$, and $\Delta = 0.38$ s, $D_{rms} = 1.53$ s, and $R = 0.54$, respectively. As Najafzadeh et al. (2024) extracted their results from a coarser grid, a certain difference from our results is expected.

We also note that we used hourly values of H_S and T_p, whereas these parameters were often recorded more frequently. This difference does not affect the quality of the match between the H_S values. However, since T_p values are more volatile, the difference in the respective procedures may lead to certain discrepancies in the T_p values.

3.4. Replication of severe wave conditions

The maximum recorded $H_S = 3.40$ m at Harilaid (Ha13; Fig. 6) was reasonably well represented by the SWAN/ERA5 suite and by the D3D suite run in stationary mode and forced with wind data from Sõrve. The SWAN/ERA5 suite is better at replicating the wave heights, but the D3D suite replicates wave periods slightly better (the bias is considerably lower). The SPM model overestimates H_S by 1 m at the peak of the wave storm on 29–30 October 2013. The overall bias and D_{rms} during the analysed period (27–31 October 2013) were 0.46 m and 0.68 m, respectively. Interestingly, the match between the recorded T_p and that reconstructed using the SPM model is even better than the match between the recorded T_p

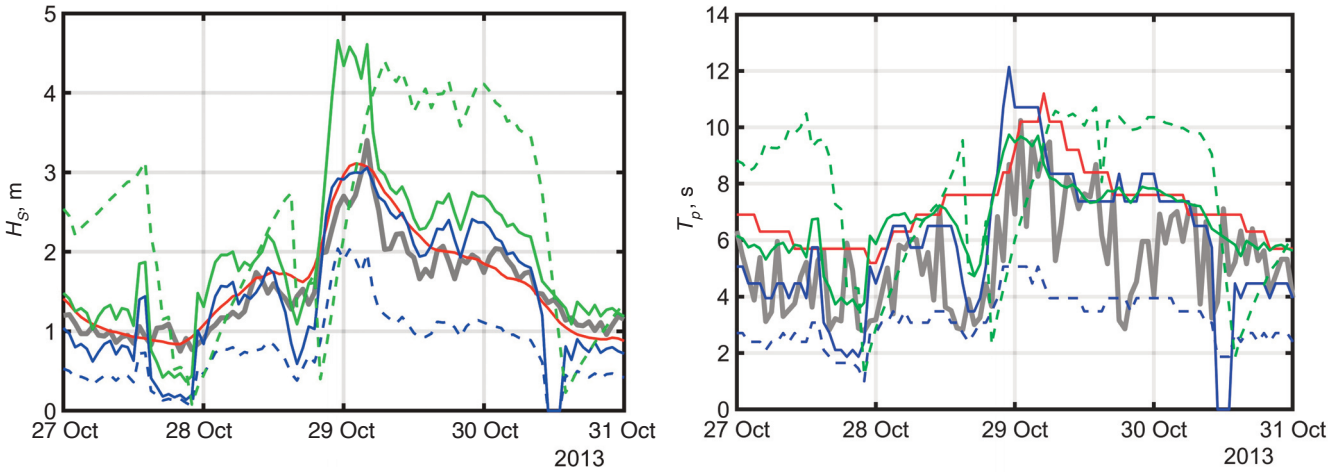

Fig. 6. Recorded (grey line) and modelled (coloured lines) H_S (left panel) and T_p (right panel) on 27–30 October 2013 at Harilaid (Ha13). Red, blue, and green lines: outputs of the SWAN/ERA5 suite, the D3D suite, and the SPM model, respectively, forced with Sõrve wind data; continuous blue and green lines: runs in stationary mode; dashed blue and green lines: runs in non-stationary mode.

and that hindcast using the SWAN/ERA5 suite. Figure 6 shows that the use of other wind data and non-stationary mode may yield substantially different values. This underlines the need to perform wave measurements and analyse the effect of different winds and modes on the results.

Both the SWAN/ERA5 and D3D suites replicate high waves ($H_S > 1$ m) very well at Kõiguste (Koi), but lower waves are clearly overestimated (Fig. 7). On the one hand, the best match with the maximum H_S is provided by the D3D suite run in stationary mode and forced with wind data from Ruhnu. On the other hand, the best statistical properties ($D_{rms} = 0.31$ m, $R = 0.91$) of the match with recorded data are provided by simulations with the SWAN/ERA5 suite. These values for the results of the D3D suite are $D_{rms} = 0.33$ m and $R = 0.83$. The use of Kihnu wind data (similar openness of the island) to force the D3D suite leads to $D_{rms} = 0.36$ m and $R = 0.51$. The SPM model overestimates H_S in both modes.

Figure 8 shows that even if the match between the modelled and recorded data is good in terms of statistical properties ($\Delta = 0.03$ m, $D_{rms} = 0.33$ m, $R = 0.75$ for the results of the D3D suite for the analysed period 27 August–2 September 2011) at Matsi (Mat), wave properties at the storm peak are not correctly represented. This feature once more suggests that the quality of the representation of extreme values, even by the very best models, should be specifically (at least visually) validated, and it is unacceptable to rely overly on statistical parameters of the match between model output and ground truth.

The course of H_S during a storm at **Kihnu** on 24–27 October 2012 (Kih; Fig. 9) demonstrates that although the best overall match among the results of runs with the D3D suite was obtained in stationary mode, forced with Kihnu wind data, the use of these most local wind data fails to depict the storm. A better match is obtained when wind data from Sõrve are used to force the model. The wind measurement stations differ in their openness to wind directions. During this storm, the recorded wind speeds at Kihnu were about two times lower than at Sõrve. The best overall match with recorded data is provided here by the SWAN/ERA5 suite, which captures the maximum H_S values well, although running the D3D suite in stationary mode and forced with Sõrve wind data gives a better match for wave heights at the storm peak. The SPM model forced with Ruhnu wind data demonstrates similar behaviour, although it is slightly overestimated compared with the hindcast of the D3D suite.

Figure 10 underlines that both the SWAN/ERA5 suite and the SPM model are unsuitable for the replication of wave heights in semi-enclosed bays such as Pärnu Bay in the north-

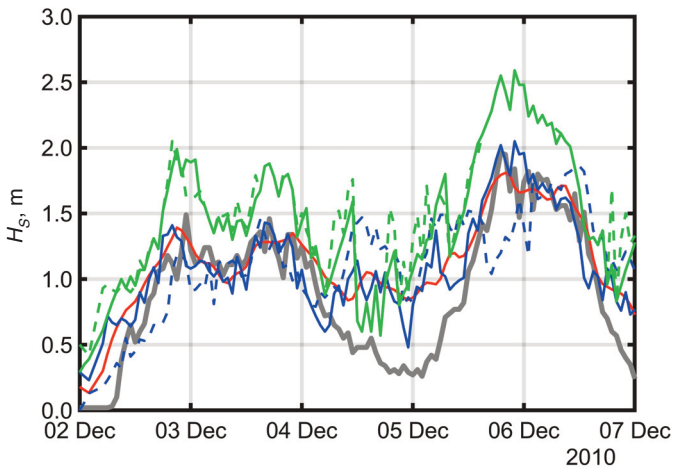

Fig. 7. Recorded (grey line) and modelled (coloured lines) H_S values on 2–7 December 2010 at Kõiguste (Koi). Red line: output of the SWAN/ERA5 suite; continuous and dashed blue lines: the D3D suite in stationary mode forced with Ruhnu and Kihnu wind data, respectively; continuous and dashed green lines: the SPM model forced with Ruhnu wind data in non-stationary and stationary modes, respectively.

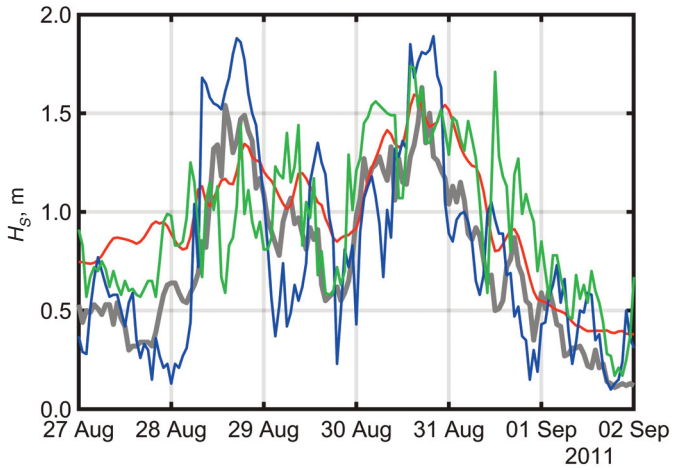

Fig. 8. Recorded (grey line) and modelled (coloured lines) H_S values on 27 August–2 September 2013 at Matsi (Mat). Red line: output of the SWAN/ERA5 suite; blue line: the D3D suite in stationary mode forced with Sõrve wind data; green line: the SPM model in stationary mode forced with Ruhnu wind data.

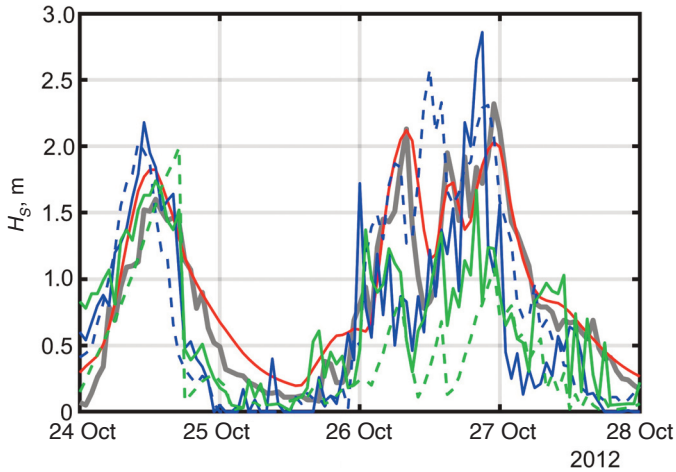

Fig. 9. Recorded (grey line) and modelled (coloured lines) H_S values on 24–28 October 2012 at Kihnu (Kih). Red line: output of the SWAN/ERA5 suite; continuous and dashed blue lines: the D3D suite in stationary mode forced with Kihnu and Sõrve wind data, respectively; continuous and dashed green lines: the SPM model forced with Ruhnu wind data in stationary and non-stationary modes, respectively.

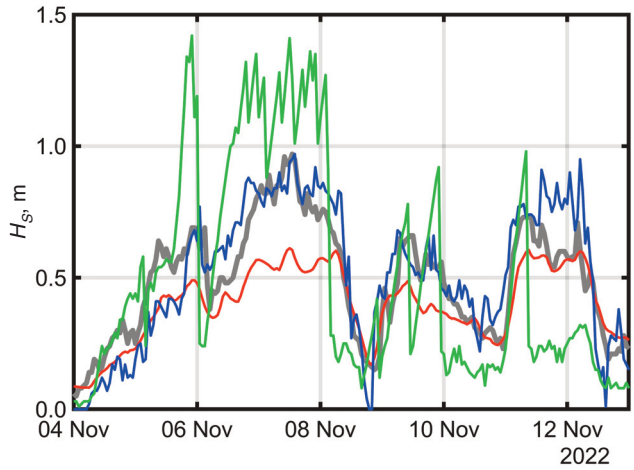

Fig. 10. Recorded (grey line) and modelled (coloured lines) H_S values on 4–12 November 2022 in Pärnu Bay (Par). Red line: output of the SWAN/ERA5 suite; blue line: the D3D suite in stationary mode forced with Kihnu wind data; green line: the SPM model in non-stationary mode forced with Ruhnu wind data.

east of the Gulf of Riga. The SWAN/ERA5 suite greatly underestimates, while the SPM model overestimates H_S. Consistent with Tõnisson et al. (2024), wave properties hindcast using the D3D suite run in non-stationary mode and forced with Kihnu wind data have the best match with recorded wave properties.

The situation is different at locations that are widely open to the sea. For example, Fig. 11 shows that the best match with recorded H_S values at locations near **Ruhnu** (Rpor and Rsea) is provided by the hindcast using the SWAN/ERA5 suite. Only the peak H_S values are slightly underestimated; however, the quality of the match is the same as, e.g., in the open part of the Gulf of Finland (Giudici et al. 2023). The performance of the D3D suite and the SPM model differ greatly between locations near Ruhnu. This difference evidently stems from the strong dependence of the estimates on the quality of the local wind data. Moreover, the SPM model cannot replicate wave refraction, which significantly contributes to wave properties near Ruhnu (Männikus et al. 2022). Although the use of wind data from Ruhnu led here and in Männikus et al. (2024a) to the best match between the modelled and recorded H_S values, waves from northern directions are severely underestimated by the model, most likely because high waves excited by northerly winds can only reach the measurement site via intense refraction.

The maximum recorded $H_S = 3.77$ m across all considered wave measurement campaigns occurred at **Skulte** (Sku; Fig. 12) in January 2022. This event was reasonably well

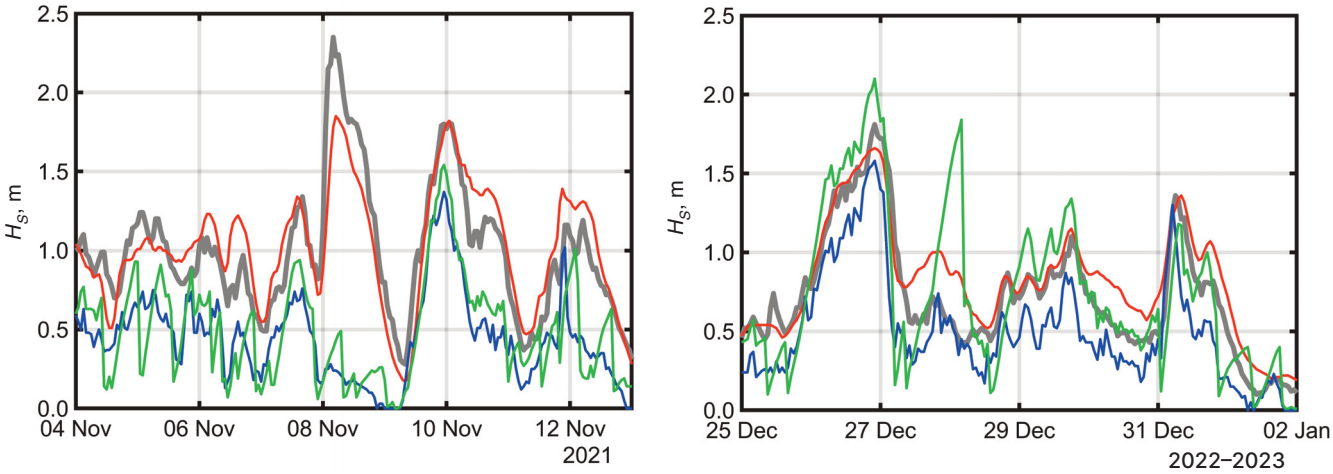

Fig. 11. Recorded (grey line) and modelled (coloured lines) H_S values near Ruhnu at Rsea (left) and Rpor (right). Red line: output of the SWAN/ERA5 suite; blue line: the D3D suite in stationary mode forced with Ruhnu wind data; green line: the SPM model in non-stationary mode forced with Ruhnu wind data.

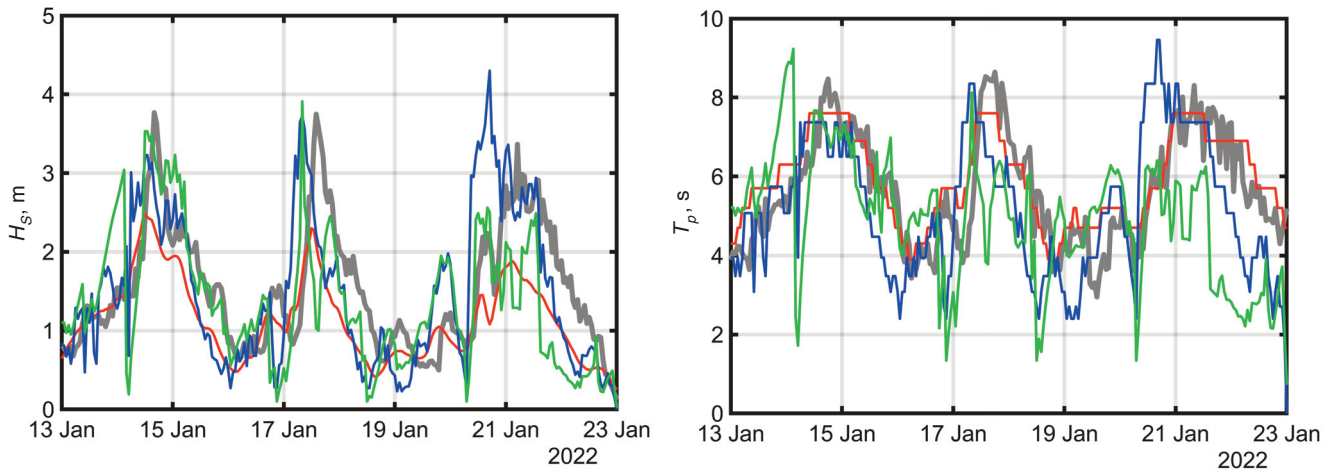

Fig. 12. Recorded (grey line) and modelled (coloured lines) H_S values (left panel) and T_p (right panel) on 13–23 January 2022 near Skulte (Sku). Red line: output of the SWAN/ERA5 suite; blue line: the D3D suite in stationary mode forced with wind data from Vilsandi; green line: the SPM model in non-stationary mode forced with wind data from Vilsandi.

represented by the D3D suite run in non-stationary mode and forced with Vilsandi wind data. Interestingly, the use of different modes results in similar hindcast wave properties. The SWAN/ERA5 suite clearly underestimates H_S, while R between the hindcast and recorded wave heights is as large as 0.80. This feature signals that relying only on correlation may lead to a misinterpretation of the performance of wave models. The reason is simple: two time series with a constant bias are perfectly correlated. The R values between the recorded H_S values and those reconstructed using the D3D suite and the SPM model are 0.62 and 0.56, respectively. The wave periods are reasonably well replicated. The SWAN/ERA5 suite has the best performance ($\Delta = 0.26$ s, $D_{rms} = 0.74$ m, and $R = 0.87$). The performance of the D3D suite and the SPM model is worse in terms of the statistical parameters used, but they still reasonably well replicate the peaks.

A series of unusually high wave conditions was recorded in October 2021 at **Rohuküla** (RoN). The maximum recorded $H_S = 3.02$ m on 23 October 2021 was omitted from the analysis since it was not recorded on the full hour. The SPM model captures the wave storm peak relatively well but clearly overestimates other values. As a consequence, the bias and D_{rms} between the modelled and recorded H_S values were larger, and R was weaker for H_S reconstructed using the SPM model than for those reconstructed using the SWAN/ERA5 and D3D suites. Likewise, the results of the SPM model depict a similar peak at RoST, but the H_S recordings are less than 0.5 m. However, as it was not a single peak, adjacent H_S values were compared with the modelling results (Fig. 13). According to EEA (2025), the 10-min average northerly wind speed exceeded 13 m/s for more than 5 h on 8 October 2023. The Port of Rohuküla is relatively well sheltered from northerly storms by several islands (Fig. 1). This is the main reason why the H_S reconstructed using the SWAN/ERA5 and D3D suites were relatively low.

A similar northerly storm was recorded on 8 October 2023. The SPM model produced very large H_S values, up to 2.5 m (Fig. 14). The wave height maxima from the SWAN/ERA5 and D3D suites, as well as from measurements, barely reached $H_S = 1$ m. This discrepancy underlines the need to carefully study local conditions when tuning fetch-based models. The D3D suite and the SPM model reasonably well repro-

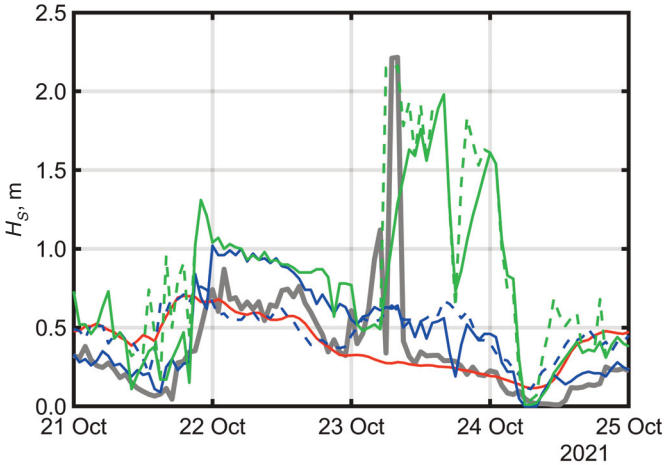

Fig. 13. Recorded (grey line) and modelled (coloured lines) H_S values on 21–25 October 2021 near Rohuküla (RoN). Red line: output of the SWAN/ERA5 suite; continuous and dashed blue lines: the D3D suite in stationary and non-stationary modes forced with Dirhami and Vilsandi wind data, respectively; continuous and dashed green lines: the SPM model forced with Dirhami wind data in stationary and non-stationary modes, respectively.

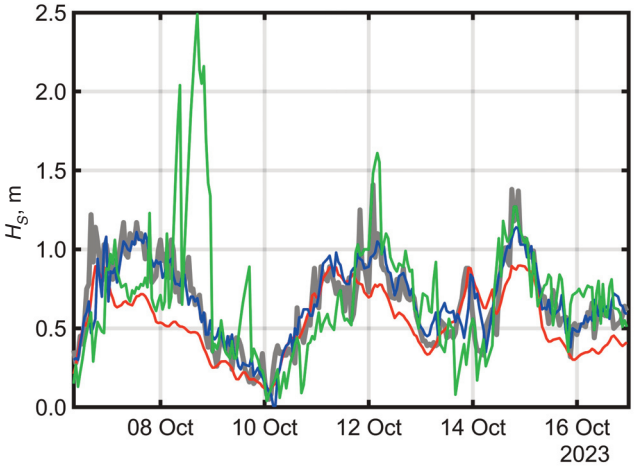

Fig. 14. Recorded (grey line) and modelled (coloured lines) H_S values on 7–16 October 2023 near Rohuküla (RoST). Red line: output of the SWAN/ERA5 suite; blue line: the D3D suite run in stationary mode forced with Osmussaar wind data; green line: the SPM model in non-stationary mode forced with Dirhami wind data.

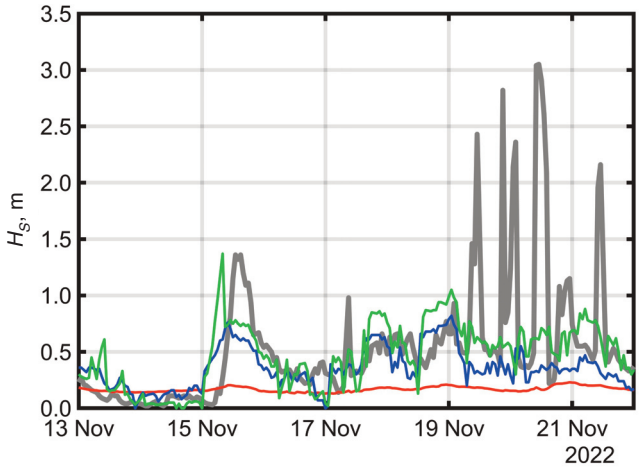

Fig. 15. Recorded (grey line) and modelled (coloured lines) H_S values on 13–21 November 2022 near Heltermaa (Hel). Red line: output of the SWAN/ERA5 suite; blue line: the D3D suite in stationary mode forced with Osmussaar wind data; green line: the SPM model in non-stationary mode forced with Osmussaar wind data.

duced the course of measured H_S values in a subsequent southwesterly storm, although the D3D suite still underestimated H_S.

As previously mentioned, recordings at **Heltermaa** (Hel) and **Kuivastu** (Kui) are affected by wave reflection and splashes, which distort the results. Although the measurement sites were carefully selected in that respect, it was almost impossible to exclude the influence of structures. This feature became evident during mild easterly winds (EEA 2025) on 19–20 November 2022, when steep peaks appeared in the H_S recordings at Heltermaa (Fig. 15). Similar peaks appeared during easterly winds at Kuivastu on 20–21 October 2023 (Fig. 16). During a northwesterly wind event, the maximum recorded H_S on 28 August 2023 was 1 m (not shown in the figures), whereas the D3D suite hindcast was only 0.7 m. However, during a northeasterly wind event >10 m/s, recordings at Heltermaa and wave heights hindcast using the SPM model were quite similar but contained a time lag of 7 h (Fig. 15). These events suggest that even when the waves do not approach perpendicular to the quay, reflection and splashes may still occur. Therefore, the recordings need careful cleaning, depending on the wave propagation direction, to properly reflect the course of approaching wave heights. Finally, the SWAN/ERA5 suite severely underestimates H_S at Heltermaa and, to some extent, at Kuivastu (Fig. 16).

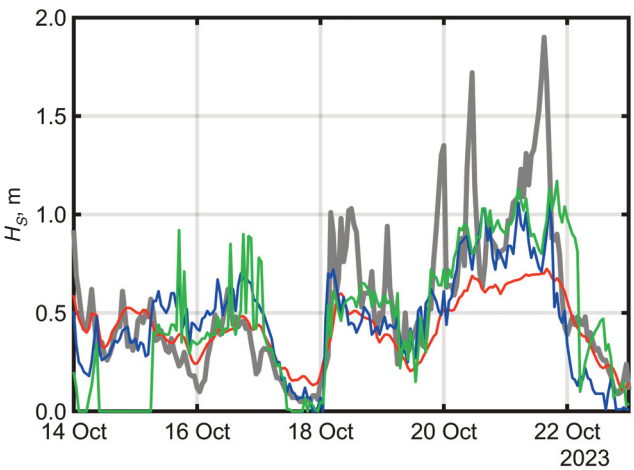

Fig. 16. Recorded (grey line) and modelled (coloured lines) H_S values on 14–22 October 2023 near Kuivastu (Kui). Red line: output of the SWAN/ERA5 suite; blue line: the D3D suite in stationary mode forced with Osmussaar wind data; green line: the SPM model in non-stationary mode forced with Osmussaar wind data.

4. Discussion

The presented data and analysis revisit the classic discussion of whether simple express models have a pertinent niche in times of big data, advanced models, digital twins, and increasing computing power. In this discussion, the argument concerning the excessive complexity of contemporary models is gradually losing its power with the rapid increase in the use of machine learning methods and artificial intelligence applications. This discussion, however, still makes sense in surface wave modelling in areas with complex bathymetry and geometry, where shortcomings in both wind information and wave models become vividly evident and where wave modelling is still a challenge. This aspect is demonstrated by taking a fresh look at the results of all available professional wave measurement campaigns in the nearshore of the Gulf of Riga, Moonsund, and the coasts of the Baltic Proper in the West Estonian Archipelago. The analysis involves the results of 15 multi-month in situ wave measurement campaigns performed in 2006–2024 at 14 nearshore locations in the eastern Baltic Sea, with a maximum duration of two years. While part of this pool of wave data has been used to calibrate and verify high-resolution wave climate simulations in the Gulf of Riga (Najafzadeh et al. 2024) and in local case studies (Männikus et al. 2024b; Tõnisson et al. 2024), more than a quarter of these datasets are considered here for the first time.

The core idea is to explore the performance of very different wave models in this area. The pool of models ranges from a multi-nested version of the SWAN wave model forced with state-of-the-art wind information from the ERA5 reanalysis (SWAN/ERA5 suite) to an almost basic parametric wave model (the SPM model) that has been slightly modified to take into account some features of the geometry of the basin. A realisation of the SWAN model in the D3D suite forced with one-point wind information from local coastal meteorological stations serves as an intermediate type of model.

Somewhat surprisingly, the SWAN/ERA5 suite tends to systematically overestimate significant wave heights. The only exceptions are Heltermaa in Moonsund, Kuivastu in the strait between Moonsund and the Gulf of Riga, and Valgerand, Pärnu Bay, and Skulte in the eastern Gulf of Riga. At Heltermaa and Kuivastu, the measurement device was mounted at a location that was prone to wave amplification owing to reflections from a vertical wall. It is natural that unexpectedly high waves are often recorded in such locations.

Part of this overestimation is apparently connected with the tendency of the SWAN/ERA5 suite to overestimate the heights of low waves. This feature mirrors the tendency of the ERA5 wind data to overestimate low wind speeds in the region (Viigand et al. 2026). This conjecture is supported by the observation that at most measurement locations, both the H_S bias and D_{rms} are smaller when only wave heights with recorded $H_S \geq 0.5$ m are considered. As relatively calm conditions occur during a large part of each year in the Baltic Sea, overestimation of wave heights during such conditions naturally translates into a bias in the parameters of the wave climate.

However, this is not the case at Skulte, Valgerand, and Pärnu, where wave fields are apparently site-specific for different reasons. The wave measurement sites at Valgerand and at another location in Pärnu Bay are sheltered from most moderate and strong winds in the region. Consequently, it is likely that wave fields at these locations are significantly influenced by refraction in the shallow Pärnu Bay during most wind conditions. It is not clear what causes such a bias at Skulte in the southeast of the Gulf of Riga, at a location that is open to one of the predominant directions of moderate and strong winds (northwest/north-northwest) in the region.

It is also notable that the magnitude of the bias and the D_{rms} of H_S of wave fields reconstructed using the D3D suite and the SPM model increases when only wave fields with $H_S \geq 0.5$ m are considered. Furthermore, the bias and D_{rms} grow only slightly if higher thresholds are applied, while R decreases significantly. This pattern signals, not unexpectedly, that both these models reproduce milder wave conditions better than intense wave events.

Interestingly, the D3D suite forced with suitably chosen wind information yields the best match with recorded wave data in relatively enclosed sub-basins (Moonsund, Pärnu Bay) and in the northern Gulf of Riga with complex bathymetry and geometry (Kõiguste, Kihnu). As already mentioned, the likely reason why the SWAN/ERA5 suite underperforms at these locations is that the ERA5 reanalysis underestimates strong winds and overestimates low winds (Viigand et al. 2026).

However, in open areas and at Kuivastu in the strait between Moonsund and the Gulf of Riga, the SWAN/ERA5 suite tends to perform better than the other options explored.

Although the SPM model uses a similar set-up to the D3D suite (homogeneous one-point wind data from coastal meteorological stations are used to run the model in stationary or non-stationary mode), its ability to replicate wave properties is very site-specific. The presented analysis signals that two types of nearshore regions are not suitable for its use. On the one hand, at locations that are fully open to the Baltic Sea, the SPM model inherently fails when the wind conditions are not homogeneous over the entire Baltic Proper. Such situations apparently constitute an overwhelming majority of all cases. On the other hand, the SPM model does not capture wave refraction and therefore also inherently fails in more sheltered, semi-enclosed areas with a notable impact of refraction (e.g. Pärnu Bay). Alternatively, the model needs further (unphysical) calibration in such cases. The performance of the SPM model in intermediate occasions, such as open areas of the Gulf of Riga and Moonsund, is not significantly worse than that of the advanced models. This feature suggests that this simple model can be used as a valuable express tool to approximately evaluate average and extreme wave properties. It is interesting that the SPM model overestimates, while the D3D suite underestimates, wave heights at Harilaid (Ha13) in the nearshore of the Baltic Proper. As the dataset from this location also contains a strong storm, examining this storm might give interesting insights into the performance of the models.

Changes in the adequacy of wave height replication can be, to a first approximation, estimated by gradually excluding lower waves from the analysis. This exercise (first excluding situations where $H_S < 0.5$ m, then $H_S < 1$ m, and $H_S < 1.5$ m) reiterates the above conjecture that the SWAN/ERA5 suite performs better than the D3D suite and the SPM model. The only exception is Heltermaa, where the measurement location itself may distort the results.

5. Conclusions

By and large, the presented analysis confirms that carefully calibrated and validated high-resolution multi-nested wave models, such as SWAN, forced with state-of-the-art modelled wind information (here, the ERA5 reanalysis) replicate basic wave properties quite well in terms of the core statistical parameters (bias, root mean square deviation, and correlation coefficient of the recorded and modelled wave heights and periods) in the nearshore areas of medium-sized water bodies, such as the Gulf of Riga and Moonsund. The spatial pattern of the match between the modelled and recorded wave properties is intriguing and instructive. On the one hand, (significant) wave heights are systematically overestimated at locations that are open to the sea (except for one location at Skulte). The bias of such estimates is smaller when only wave fields with $H_S \geq 0.5$ m are considered. On the other hand, wave heights in more enclosed areas (Moonsund, Pärnu Bay) are slightly underestimated, while the situation is reversed when only waves exceeding a higher threshold are considered. Peak wave heights in storms (near Ruhnu, at Skulte, in Moonsund, and in Pärnu Bay) are severely underestimated. These features together suggest that ERA5 winds do not adequately replicate strong wind patterns in the region.

Another conclusion is that different locations may need different tuning of wave model parameters. The relevant analysis for Pärnu Bay signals that substantial modifications may be needed at some locations. Wave heights were underestimated at Skulte, but generally well replicated at other locations in the Gulf of Riga. This feature suggests that it may not be sufficient to rely on calibration and validation conducted at another location in the same water body.

Intriguingly, wave models forced with recorded one-point wind properties (especially the SWAN-based D3D suite) performed better in medium-sized semi-enclosed areas. Their performance was also good in strong storms, where the peaks were adequately represented, although sometimes with a time lag. Thus, it may be reasonable to apply contemporary wave models with a default set-up but forced with locally recorded one-point wind information from unsheltered locations to estimate the properties of extreme waves in the Gulf of Riga. In this context, wind data from Dirhami at the entrance to the Gulf of Finland may serve as a suitable source even though the wind measurement site is sheltered from the west by forest.

Interestingly, the D3D suite and the SPM model run in stationary mode often perform better than these models run in non-stationary mode. This is especially the case for the D3D suite. Still, the SPM model run in non-stationary mode performs better in semi-enclosed areas, such as Moonsund and Pärnu Bay. It is likely that fine-tuned site-specific models work better in non-stationary mode; however, this feature needs further study.

As expected, the SWAN/ERA5 suite replicates the recorded peak periods T_p better than the other models at almost all locations in terms of bias, D_{rms}, and R. The periods T_p hindcast with the D3D suite have a slightly better match with recorded data in Moonsund. A possible reason is that wave fields in this smaller water body are often fully developed. This conjecture is supported by the relatively low bias of T_p evaluated using the SPM model. At some locations, these values were even smaller than those for the results of the D3D and SWAN/ERA5 suites. However, D_{rms} values for the results of the SPM model are higher, and R values lower, than the corresponding quantities for the other models. There is no clear pattern among the models as to where the peak periods are overestimated.

Interestingly, the match between recorded wave periods and those replicated using the SWAN/ERA5 and D3D models (and the SPM model at some locations) does not improve when only higher waves are taken into account. The relevant statistical parameters of the match remain almost unchanged, which corresponds well with findings in Männikus et al. (2024a). The only exception is at Rohuküla (RoS), where the correlation of wave periods at a threshold of $H_S \geq 0.5$ m ($R = 0.77$) is much stronger than for all waves ($R = 0.3$). This signals that low waves recorded using a pressure sensor may have erroneously long periods.

As a local feature, our analysis shows that measuring waves with an echosounder mounted on the top of vertical structures may lead to deceptive results because of wave–structure interactions at some approach directions. Therefore, it is necessary to carefully filter out reflections and splashes from the recordings. Here, simple wave models could be of great value.

For practical purposes, it seems safe to use simple one-point wind data to force the SWAN or WAM model for rapid estimates of design parameters. However, the results should be interpreted in the light of established deficiencies in the accurate estimation of wave periods.

In conclusion, the presented analysis suggests that simplified techniques, and in particular the use of high-quality one-point marine wind data, still have a clear niche in rapid estimates of average and extreme wave parameters in semi-sheltered areas with complex bathymetry and geometry. This conjecture essentially reflects challenges in the replication of wind forcing over such basins as the Baltic Sea (e.g. Lorenz and Gräwe 2023) rather than the complexity and/or computational costs of contemporary wave models. Another core message is that such simpler models need careful calibration against wave measurements at a nearby location to select the appropriate model type and wind forcing.

Data availability statement

Data are contained within the article.

Acknowledgements

The research was co-supported by the Estonian Research Council (grants PRG1129, PRG3038, and PRG1471), the Clean Energy Transition Partnership (CETPartnership) project FROST (via the Estonian Research Council subgrant MOB3PRT25), and Tallinn University of Technology (TalTech) bridging grant GFLTRM25. Rain Männikus acknowledges support from Saarte Liinid AS under contract LTEE21048 with TalTech. The authors are grateful to Māris Skudra for providing wave recordings from Skulte. The publication costs of this article were partially covered by the Estonian Academy of Sciences.

Appendix

Details of wave measurements

A recording (Acoustic) Doppler Current Profiler RDCP-600 was used at five analysed locations (Fig. 1; Fig. A1; Table 2) in 2006–2013 (e.g. Suursaar et al. 2012; Suursaar 2015). The autonomous, upward-looking instrument was installed on the seabed by divers, typically at a distance of 1–2 km from the shoreline at a depth of 10–13 m. The recording interval of 1 h matches the temporal resolution of routinely measured meteorological data used in wave model calibrations and hindcasts. Wave parameters were evaluated in these campaigns using a high-precision quartz pressure sensor with a resolution of 0.001% of full scale (Suursaar and Kullas 2009). The significant wave height H_S and an estimate of wave periods were calculated internally by the device based on the energy spectrum.

Time series of wave properties were recorded near the Port of Rohuküla in 2021–2022 using self-logging devices called hydromasts (Ristolainen et al. 2019; Egerer et al. 2024; Eelsalu et al. 2025). The loggers, manufactured by the Centre of Biorobotics at Tallinn University of Technology, recorded pressure fluctuations at a frequency of 5 Hz at a depth of 4 m at two locations (RoN and RoS in Fig. A2). The duration of each deployment was approximately 1.5 months, constrained by battery capacity. The measurements were performed only during the navigation seasons of 2021 and 2022. Pressure records were first transformed into water level fluctuations, after which significant wave heights (H_S) and wave periods were computed at 15-min intervals using MATLAB routines following Karimpour (2013).

A directional waverider LainePoiss® produced by WiseParker Ltd (Alari et al. 2022) was deployed near the Port of Ruhnu (Fig. A3) and in Pärnu Bay (Fig. A4) in 2021–2023. This is a surface-following buoy with a diameter of 32 cm, a height of 22 cm, and a weight of 3.5 kg. The LainePoiss® data stream has been comprehensively validated through (i) laboratory sensor testing, (ii) controlled wave flume experiments, (iii) field comparisons with an industrial Directional Waverider, (iv) intercomparisons among multiple buoys de-

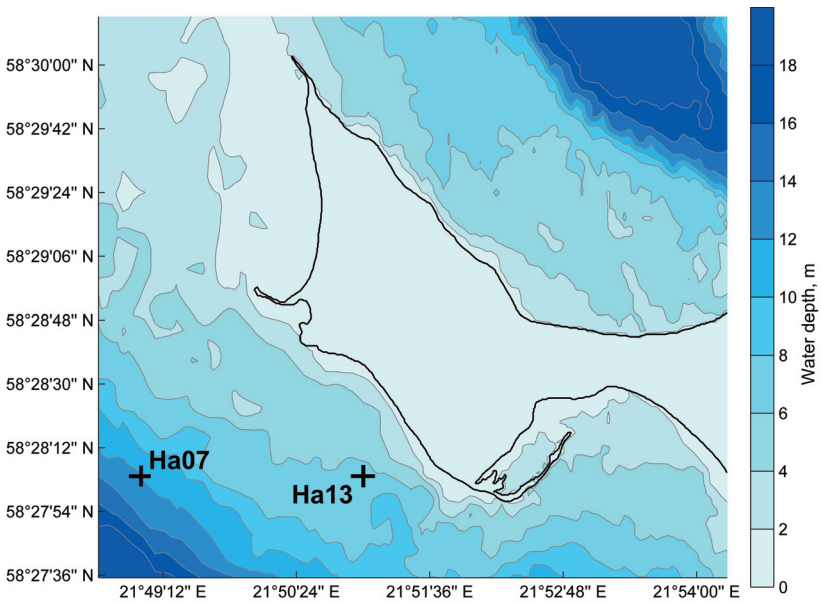

Fig. A1. Measurement locations (crosses) near the Harilaid Peninsula.

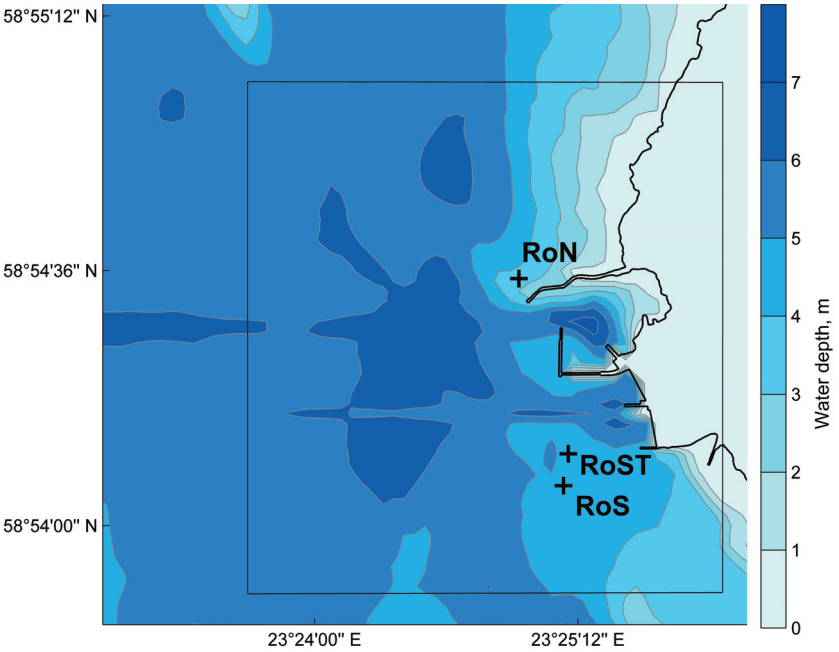

Fig. A2. Measurement locations (crosses) near the Port of Rohuküla. The thin black square indicates the Rohuküla grid boundaries (Table 1).

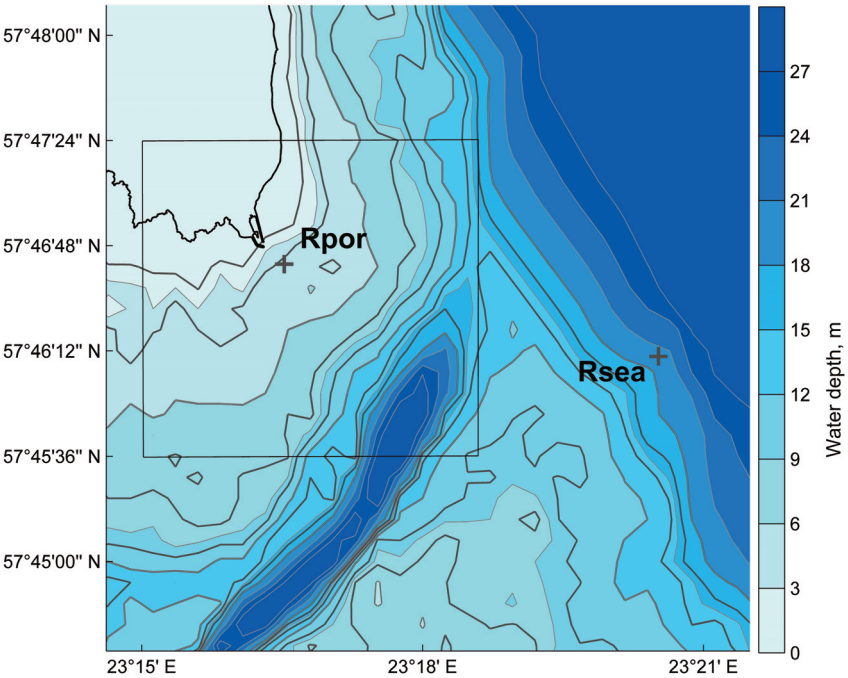

Fig. A3. Measurement locations near the island of Ruhnu. The thin black square indicates the Ruhnu grid boundaries (Table 1).

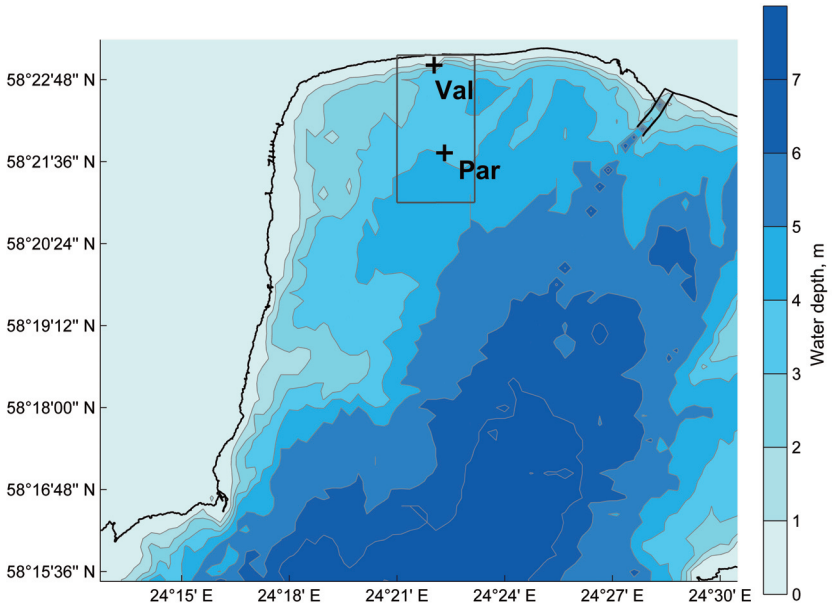

Fig. A4. Measurement locations in Pärnu Bay. The thin black rectangle indicates the Valgerand grid boundaries (Table 1).

Photo A1. Echosounder at Heltermaa. Photo by Rain Männikus.

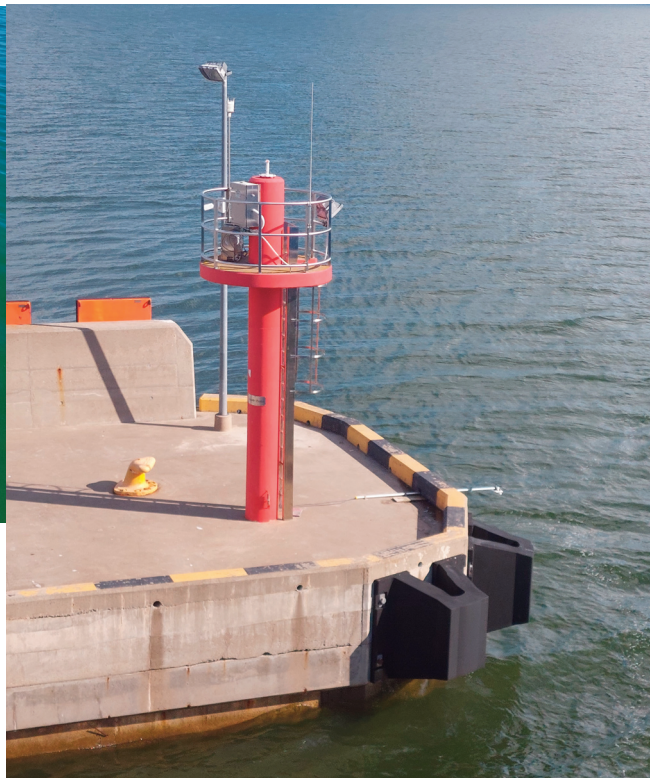

Photo A2. Echosounder at Kuivastu. Photo by Rain Männikus.

ployed in situ, and (v) field observations in the Baltic Sea marginal ice zone (Alari et al. 2022). The bias of H_S was 1 cm, with a correlation coefficient of 0.99 and a scatter index of 8% compared with the output of similar devices. The mean absolute deviation of the mean wave direction was 70°. The measurements are described in more detail in Männikus et al. (2024b) and Tõnisson et al. (2024).

A Taiwanese directional waverider produced by Driftertek was used in 2023 to record wave properties near Rohuküla (RoST in Fig. A2). This is a spherical buoy with a diameter of 50 cm, a height of 32 cm, and a weight of 5 kg. Finally, high-resolution echosounders (LOG_aLevel® devices, General Acoustics, Kiel, Germany) were mounted at the eastern ends of the quays of the Port of Heltermaa (Photo A1) and Port of Kuivastu (Photo A2). The sensors were about 3.6 m above mean sea level. According to the manufacturer, the measurement range of the sensors is 0.5–10 m, with a resolution of ±1 mm for single measurements.

References

Adell, A., Almström, B., Kroon, A., Larson, M., Uvo, C. B. and Hallin, C. 2023. Spatial and temporal wave climate variability along the south coast of Sweden during 1959–2021. *Regional Studies in Marine Science*, **63**, 103011. https://doi.org/10.1016/j.rsma.2023.103011

Afolabi, L. A., Russo, S., Re, C. L., Ludeno, G., Nardone, G., Vicinanza, D. et al. 2025. Underestimation of wave energy from ERA5 datasets: back analysis and calibration in the Central Tyrrhenian Sea. *Energies*, **18**(1), 3. https://doi.org/10.3390/en18010003

Alari, V., Björkqvist, J.-V., Kaldvee, V., Mölder, K., Rikka, S., Kask-Korb, A. et al. 2022. LainePoiss® – a lightweight and ice-resistant wave buoy. *Journal of Atmospheric and Oceanic Technology*, **39**(5), 573–594. https://doi.org/10.1175/JTECH-D-21-0091.1

Andrée, E., Su, J., Dahl Larsen, M. A., Drews, M., Stendel, M. and Skovgaard Madsen, K. 2023. The role of preconditioning for extreme storm surges in the western Baltic Sea. *Natural Hazards and Earth System Sciences*, **23**(5), 1817–1834. https://doi.org/10.5194/nhess-23-1817-2023

Barbariol, F., Davison, S., Falcieri, F. M., Ferretti, R., Ricchi, A., Sclavo, M. et al. 2021. Wind waves in the Mediterranean Sea: an ERA5 reanalysis wind-based climatology. *Frontiers in Marine Science*, **8**, 760614. https://doi.org/10.3389/fmars.2021.760614

Bessonova, V., Tapoglou, E., Dorrell, R., Dethlefs, N. and York, K. 2025. Global evaluation of wave data reanalysis: comparison of the ERA5 dataset to buoy observations. *Applied Ocean Research*, **157**, 104490. https://doi.org/10.1016/j.apor.2025.104490

Björkqvist, J.-V., Tuomi, L., Fortelius, C., Pettersson, H., Tikka, K. and Kahma, K. K. 2017. Improved estimates of nearshore wave conditions in the Gulf of Finland. *Journal of Marine Systems*, **171**, 43–53. https://doi.org/10.1016/j.jmarsys.2016.07.005

Björkqvist, J.-V., Lukas, I., Alari, V., van Vledder, G. P., Hulst, S., Pettersson, H. et al. 2018. Comparing a 41-year model hindcast with decades of wave measurements from the Baltic Sea. *Ocean Engineering*, **152**, 57–71. https://doi.org/10.1016/j.oceaneng.2018.01.048

Björkqvist, J.-V., Rikka, S., Alari, V., Männik, A., Tuomi, L. and Pettersson, H. 2020. Wave height return periods from combined measurement – model data: a Baltic Sea case study. *Natural Hazards and Earth System Science*, **20**(12), 3593–3609. https://doi.org/10.5194/nhess-20-3593-2020

Booij, N., Ris, R. C. and Holthuijsen, L. H. 1999. A third-generation wave model for coastal regions: 1. Model description and validation. *Journal of Geophysical Research: Oceans*, **104**(C4), 7649–7666. https://doi.org/10.1029/98JC02622

Borsche, M., Kaiser-Weiss, A. K. and Kaspar, F. 2016. Wind speed variability between 10 and 116 m height from the regional reanalysis COSMO-REA6 compared to wind mast measurements over northern Germany and the Netherlands. *Advances in Science and Research*, **13**, 151–161. https://doi.org/10.5194/asr-13-151-2016

BSHC (Baltic Sea Hydrographic Commission). 2013. *Baltic Sea Bathymetry Database version 0.9.3*. https://www.bshc.pro/data (accessed 2020-02-15).

Caliskan, H. and Valle-Levinson, A. 2008. Wind-wave transformations in an elongated bay. *Continental Shelf Research*, **28**(14), 1702–1710. https://doi.org/10.1016/j.csr.2008.03.009

Didenkulova, I. 2011. Shapes of freak waves in the coastal zone of the Baltic Sea (Tallinn Bay). *Boreal Environment Research*, **16**(Suppl. A), 138–148.

ECMWF (European Centre for Medium-Range Weather Forecasts). 2016. IFS documentation Cy41r2 – part IV: physical processes. In *IFS Documentation CY41R2*. ECMWF, Reading. https://www.ecmwf.int/en/elibrary/79697-ifs-documentation-cy41r2-part-iv-physical-processes (accessed 2023-02-07).

EEA (Estonian Environment Agency). 2025. *Ajaloolised ilmaandmed* (*Historical weather data*). https://www.ilmateenistus.ee/kliima/ajaloolised-ilmaandmed/ (accessed 2025-07-01).

Eelsalu, M. and Soomere, T. 2026. Disruptions in alongshore sediment transport on sedimentary shores of the Baltic Sea driven by changes in forcing wave fields. *Ocean Engineering*, **356**(1), 124952. https://doi.org/10.1016/j.oceaneng.2026.124952

Eelsalu, M., Piho, L., Aigars, J., Kelpšaitė-Rimkienė, L., Kondrat, V., Kruusmaa, M. et al. 2025. Exponential distribution of wave-driven near-bed water speeds under short-crested waves: a case study in the eastern Gulf of Riga, the Baltic Sea. *Proceedings of the Estonian Academy of Sciences*, **74**(1), 23–42. https://doi.org/10.3176/proc.2025.1.03

Egerer, M., Ristolainen, A., Piho, L., Vihman, L. and Kruusmaa, M. 2024. Hall effect sensor-based low-cost flow monitoring device: design and validation. *IEEE Sensors Journal*, **24**(5), 5986–5997. https://doi.org/10.1109/JSEN.2024.3354194

Gandoin, R. and Garza, J. 2024. Underestimation of strong wind speeds offshore in ERA5: evidence, discussion and correction. *Wind Energy Science*, **9**(8), 1727–1745. https://doi.org/10.5194/wes-9-1727-2024

Giudici, A., Jankowski, M. Z., Männikus, R., Najafzadeh, F., Suursaar, Ü. and Soomere, T. 2023. A comparison of Baltic Sea wave properties simulated using two modelled wind data sets. *Estuarine, Coastal and Shelf Science*, **290**, 108401. https://doi.org/10.1016/j.ecss.2023.108401

Groll, N. and Weisse, R. 2017. A multi-decadal wind-wave hindcast for the North Sea 1949–2014: coastDat2. *Earth System Science Data*, **9**(2), 955–968. https://doi.org/10.5194/essd-9-955-2017

Hanes, D. M. and Erikson, L. H. 2013. The significance of ultra-refracted waves on sheltered coasts, with application to San Francisco Bay. *Estuarine, Coastal, and Shelf Science*, **133**, 129–136. https://doi.org/10.1016/j.ecss.2013.08.022

Hersbach, H., Bell, B., Berrisford, P., Biavati, G., Horányi, A., Muñoz Sabater, J. et al. 2018. ERA5 hourly data on pressure levels from 1940 to present. *Copernicus Climate Change Service (C3S) Climate Data Store (CDS)*. https://doi.org/10.24381/cds.bd0915c6 (accessed 2023-09-01).

Hersbach, H., Bell, B., Berrisford, P., Hirahara, S., Horányi, A., Muñoz-Sabater, J. et al. 2020. The ERA5 global reanalysis. *Quarterly Journal of the Royal Meteorological Society*, **146**(730), 1999–2049. https://doi.org/10.1002/qj.3803

Huttula, T. 1994. Suspended sediment transport in Lake Säkylän Pyhäjärvi. *Aqua Fennica*, **24**(2), 171–185.

Kamphuis, J. W. 2010. Introduction to Coastal Engineering and Management. 2nd ed. World Scientific, Singapore.

Karimpour, A. 2013. *OCEANLYZ, Ocean Wave Analyzing Toolbox. User manual*. http://www.arashkarimpour.com/download.html (accessed 2026-03-23).

Keevallik, S. 2003. Possibilities of reconstruction of the wind regime over Tallinn Bay. *Proceedings of the Estonian Academy of Sciences. Engineering*, **9**(3), 209–219. https://doi.org/10.3176/eng.2003.3.04

Keevallik, S., Soomere, T., Pärg, R. and Žukova, V. 2007. Outlook for wind measurement at Estonian automatic weather stations. *Proceedings of the Estonian Academy of Sciences. Engineering*, **13**(3), 234–251. https://doi.org/10.3176/eng.2007.3.05

LEGMC (Latvian Environment, Geology and Meteorology Centre). 2025. Environmental data archive. Meteorology. https://videscentrs.lvgmc.lv/noverojumu-arhivs/meteo (accessed 2025-12-27).

Lorenz, M. and Gräwe, U. 2023. Uncertainties and discrepancies in the representation of recent storm surges in a non-tidal semi-enclosed basin: a hindcast ensemble for the Baltic Sea. *Ocean Science*, **19**(6), 1753–1771. https://doi.org/10.5194/os-19-1753-2023

Lu, B. Y., Wang, W., Wu, C. and Liu, Y. L. 2026. Wave climate on the southwestern coast of Lake Michigan: perspectives from wave directionality. *Ocean Engineering*, **343**(2), 123306. https://doi.org/10.1016/j.oceaneng.2025.123306

Männikus, R. and Soomere, T. 2023. Directional variation of return periods of water level extremes in Moonsund and in the Gulf of Riga, Baltic Sea. *Regional Studies in Marine Science*, **57**, 102741. https://doi.org/10.1016/j.rsma.2022.102741

Männikus, R., Soomere, T. and Viška, M. 2020. Variations in the mean, seasonal and extreme water level on the Latvian coast, the eastern Baltic Sea, during 1961–2018. *Estuarine, Coastal and Shelf Science*, **245**, 106827. https://doi.org/10.1016/j.ecss.2020.106827

Männikus, R., Soomere, T. and Najafzadeh, F. 2022. Refraction may redirect waves from multiple directions into a harbour: a case study in the Gulf of Riga, eastern Baltic Sea. *Estonian Journal of Earth Sciences*, **71**(2), 80–88. https://doi.org/10.3176/earth.2022.06

Männikus, R., Soomere, T. and Suursaar, Ü. 2024a. How do simple wave models perform compared with sophisticated models and measurements in the Gulf of Finland? *Estonian Journal of Earth Sciences*, **73**(2), 98–111. https://doi.org/10.3176/earth.2024.10

Männikus, R., Wang, W. W., Eelsalu, M., Najafzadeh, F., Bihs, H. and Soomere, T. 2024b. Modelling suitable layout for a small island harbour: a case study of Ruhnu in the Gulf of Riga, eastern Baltic Sea. *Latvian Journal of Physics and Technical Sciences*, **61**(6), 3–24. https://doi.org/10.2478/lpts-2024-0040

Massel, S. R. 2013. *Ocean Surface Waves: Their Physics and Prediction*. 2nd ed. World Scientific, Singapore.

Najafzadeh, F., Jankowski, M. Z., Giudici, A., Männikus, R., Suursaar, Ü., Viška, M. et al. 2024. Spatiotemporal variability of wave climate in the Gulf of Riga. *Oceanologia*, **66**(1), 56–77. https://doi.org/10.1016/j.oceano.2023.11.001

Pettersson, H., Kahma, K. K. and Tuomi, L. 2010. Wave directions in a narrow bay. *Journal of Physical Oceanography*, **40**(1), 155–169. https://doi.org/10.1175/2009JPO4220.1

Pettersson, H., Lindow, H. and Brüning, T. 2013. Wave climate in the Baltic Sea 2012. *HELCOM Baltic Sea Environment Fact Sheets 2013*.

Ridal, M., Olsson, E., Unden, P., Zimmermann, K. and Ohlsson, A. 2017. *Uncertainties in Ensembles of Regional Re-Analyses–Deliverable D2*. 7 HARMONIE Reanalysis Report of Results and Dataset. SMHI, Norrköping.

Ristolainen, A., Tuhtan, J. A. and Kruusmaa, M. 2019. Continuous, near-bed current velocity estimation using pressure and inertial sensing. *IEEE Sensors Journal*, **19**(24), 12398–12406. https://doi.org/10.1109/JSEN.2019.2937954

Salonen, N. and Rautenbach, C. 2021. Toward nearshore, bathymetry induced wave amplification in False Bay, South Africa. *AIP Advances*, **11**(7), 075209. https://doi.org/10.1063/5.0055734

Seymour, R. J. 1977. Estimating wave generation on restricted fetches. *Journal of the Waterway, Port, Coastal and Ocean Division*, **103**(2), 251–263. https://doi.org/10.1061/JWPCDX.0000026

She, J., Meier, H. E. M., Darecki, M., Gorringe, P., Huess, V., Kõuts, T. et al. 2020. Baltic Sea operational oceanography – a stimulant for regional Earth system research. *Frontiers in Earth Science*, **8**(7). https://doi.org/10.3389/feart.2020.00007

Sheridan, L. M., Krishnamurthy, R., García Medina, G., Gaudet, B. J., Gustafson, W. I., Jr., Mahon, A. M. et al. 2022. Offshore reanalysis wind speed assessment across the wind turbine rotor layer off the United States Pacific coast. *Wind Energy Science*, **7**(5), 2059–2084. https://doi.org/10.5194/wes-7-2059-2022

Skudra, M. and Lips, U. 2017. Characteristics and inter-annual changes in temperature, salinity and density distribution in the Gulf of Riga. *Oceanologia*, **59**(1), 37–48. https://doi.org/10.1016/j.oceano.2016.07.001

Soomere, T. 2001. Wave regimes and anomalies off north-western Saaremaa Island. *Proceedings of the Estonian Academy of*

Sciences. Engineering, **7**(2), 157–173. https://doi.org/10.3176/eng.2001.2.06

Soomere, T. 2003. Anisotropy of wind and wave regimes in the Baltic proper. *Journal of Sea Research*, **49**(4), 305–316. https://doi.org/10.1016/S1385-1101(03)00034-0

Soomere, T. 2005. Wind wave statistics in Tallinn Bay. *Boreal Environment Research*, **10**(2), 103–118. https://doi.org/10.60910/ycqv-t4wd

Soomere, T. 2023. Numerical simulations of wave climate in the Baltic Sea: a review. *Oceanologia*, **65**(1), 117–140. https://doi.org/10.1016/j.oceano.2022.01.004

Soomere, T. and Eelsalu, M. 2014. On the wave energy potential along the eastern Baltic Sea coast. *Renewable Energy*, **71**, 221–233. https://doi.org/10.1016/j.renene.2014.05.025

Soomere, T. and Räämet, A. 2011. Long-term spatial variations in the Baltic Sea wave fields. *Ocean Science*, **7**(1), 141–150. https://doi.org/10.5194/os-7-141-2011

Soomere, T. and Rannat, K. 2003. An experimental study of wind waves and ship wakes in Tallinn Bay. *Proceedings of the Estonian Academy of Sciences. Engineering*, **9**(3), 157–184. https://doi.org/10.3176/eng.2003.3.02

Soomere, T., Behrens, A., Tuomi, L. and Nielsen, J. W. 2008. Wave conditions in the Baltic Proper and in the Gulf of Finland during windstorm Gudrun. *Natural Hazards and Earth System Sciences*, **8**(1), 37–46. https://doi.org/10.5194/nhess-8-37-2008

Soomere, T., Pindsoo, K., Kudryavtseva, N. and Eelsalu, M. 2020. Variability of distributions of wave set-up heights along a shoreline with complicated geometry. *Ocean Science*, **16**(5), 1047–1065. https://doi.org/10.5194/os-16-1047-2020

Stiebrins, O. and Väling, P. 1996. *Bottom Sediments of the Gulf of Riga*. Geological Survey of Latvia, Riga.

Suursaar, Ü. 2013. Locally calibrated wave hindcasts in the Estonian coastal sea in 1966–2011. *Estonian Journal of Earth Sciences*, **62**(1), 42–56. https://doi.org/10.3176/earth.2013.05

Suursaar, Ü. 2015. Analysis of wave time series in the Estonian coastal sea in 2003–2014. *Estonian Journal of Earth Sciences*, **64**(4), 289–304. https://doi.org/10.3176/earth.2015.35

Suursaar, Ü. and Kullas, T. 2009. Decadal variations in wave heights off Cape Kelba, Saaremaa Island, and their relationships with changes in wind climate. *Oceanologia*, **51**(1), 39–61. https://doi.org/10.5697/oc.51-1.039

Suursaar, Ü., Kullas, T. and Aps, R. 2012. Currents and waves in the northern Gulf of Riga: measurement and long-term hindcast. *Oceanologia*, **54**(3), 421–447. https://doi.org/10.5697/oc.54-3.421

Suursaar, Ü., Alari, V. and Tõnisson H. 2014. Multi-scale analysis of wave conditions and coastal changes in the north-eastern Baltic Sea. *Journal of Coastal Research*, **70**(sp1), 223–228. https://doi.org/10.2112/SI70-038.1

Tolvanen, H. and Suominen, T. 2005. Quantification of openness and wave activity in archipelago environments. *Estuarine, Coastal and Shelf Science*, **64**(2–3), 436–446. https://doi.org/10.1016/j.ecss.2005.03.001

Tõnisson, H., Männikus, R., Kont, A., Palginõmm, V., Alari, V., Suuroja, S. et al. 2024. Application of shore sediments accumulated in navigation channel for restoration of sandy beaches around Pärnu city, SW Estonia, Baltic Sea. *Journal of Marine Science and Engineering*, **12**(3), 394. https://doi.org/10.3390/jmse12030394

Tsyrulnikov, A., Tuuling, I. and Hang, T. 2008. Streamlined topographical features in and around the Gulf of Riga as evidence of Late Weichselian glacial dynamics. *Geological Quarterly*, **52**(1), 81–89.

USACE (U.S. Army Corps of Engineers). 1984. *Shore Protection Manual*. Vol. 1, 3rd ed. U.S. Government Printing Office, Washington D.C.

Viigand, K., Giudici, A., Männikus, R. and Soomere, T. 2026. Wind properties in the Gulf of Riga: a comparison of modelled and measured data. *Oceanologia*, under review.

WAVE. 2013. *Delft3D-WAVE User Manual*. 3.03 ed. Deltares, Delft.

Wu, J. 1982. Wind-stress coefficients over sea surface from breeze to hurricane. *Journal of Geophysical Research*, **87**(C12), 9704–9706. https://doi.org/10.1029/JC087iC12p09704

Žukova, V. 2009. *Eesti rannikujaamade võimalused meretuule hindamisel (Possibilities of estimation of marine winds from Estonian coastal stations)*. MSc thesis. Tallinn University of Technology, Estonia.

Kus saab Liivi lahes kasutada lihtsaid lainemudeleid keerukate asemel?

Rain Männikus, Tarmo Soomere, Ülo Suursaar ja Hwa Chien

Lainetuse parameetrid on rannikul ja merel paiknevate rajatiste projekteerimisel võtmetähtsusega. Nende mõõtmine ja analüüs on aga aeganõudev ja kallis, mistõttu tihti soovitakse praktikas otsustamiseks kiiret, kuid siiski adekvaatset hinnangut. Selleks on eri aegadel tarvitatud väga erinevaid mudeleid, alates nn parameetrilistest (mereala suuruse ehk tuule jooksumaa ja kohaliku tuule omaduste alusel lainetuse omadusi hindavatest) mudelitest kuni nüüdisaegsete kõrglahutusega tuuleinfot rakendavate täisspektraalsete lainemudeliteni, nagu WAM või SWAN. Käesolevas töös võrdleme kolme erinevat tüüpi mudeli pakutavat laineinfot Liivi lahes ja Väinameres neljateistkümnes kohas mõõdetud lainetuse omadustega. Uurime, (i) millised mõõdetud tuuleandmed ja milline mudeli töörežiim (statsionaarne/mittestatsionaarne) sobivad lainetuse parameetrite arvutamiseks, (ii) kas lihtsad parameetrilised mudelid töötavad piisavalt hästi, et anda lainetuse kohta mõistlik kiirhinnang, ning (iii) kas on kohti, kus mõnda tüüpi mudel ei saa üldse hakkama. Tulemused näitasid, et ühest punktist kogu mudelialale rakendatud kvaliteetne tuuleinfo annab paljudes kohtades (Väinameri, Pärnu laht, Skulte) paremaid tulemusi kui kõrglahutusega (nt ERA5 andmestikul põhinev) tuuleinfo. Keskne järeldus kordab klassikalisi sõnumeid: lainetuse omaduste rekonstruktsiooni headuse määravad eelkõige kasutatud tuuleinfo kvaliteet ning võimalus võrrelda modelleeritud lainetuse parameetreid mõõtmistulemustega.